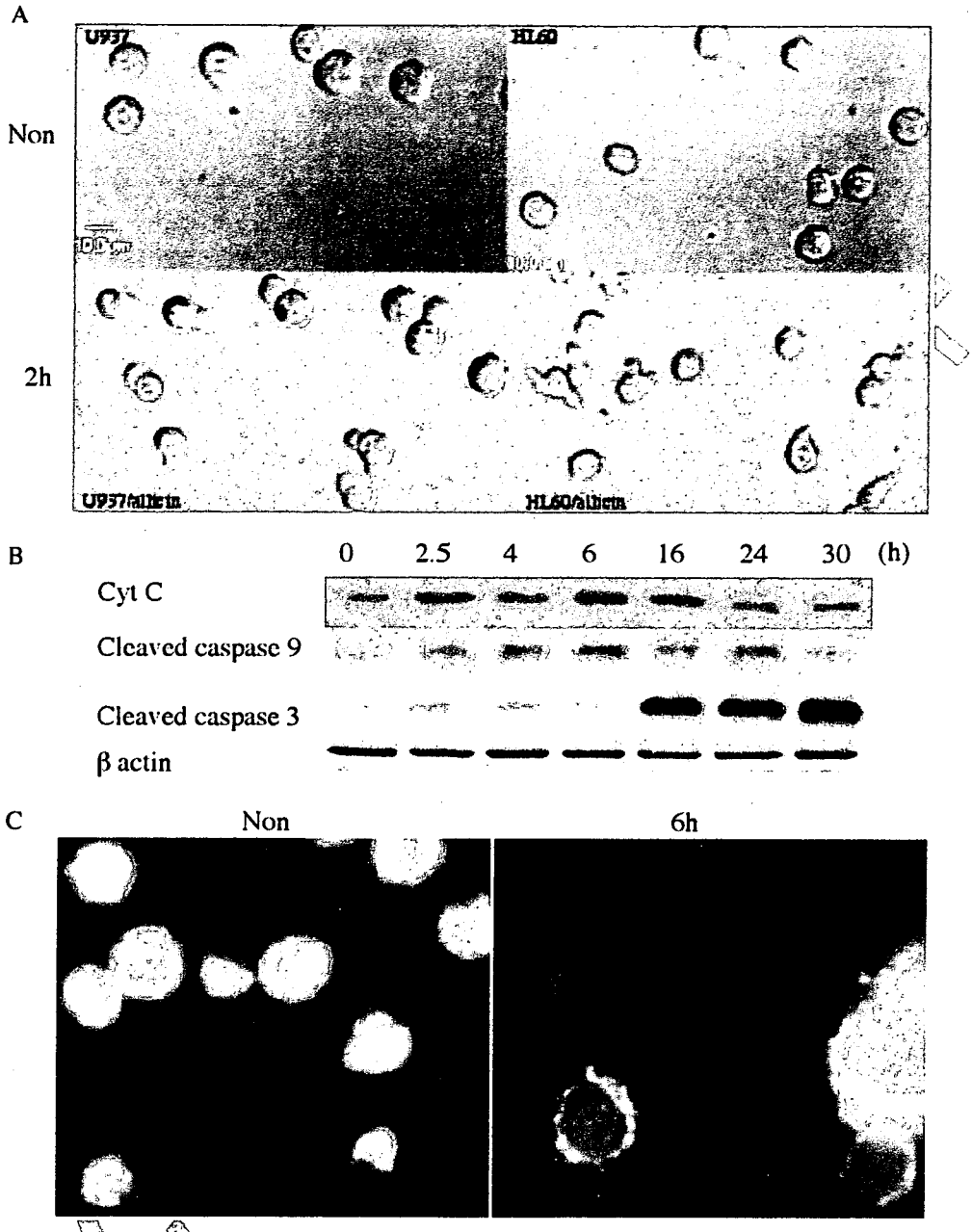

Fig. 3. (A) Morphological changes in HL60 and U937cells treated with allicin. HL60 and U937 cells treated with allicin (5 or 20 μM, respectively) for 2 h were collected and washed with PBS. Cells were visualized by confocal microscopy (original magnification ×40). (Upper panel) Nontreated cells (the diameter of 100 cells was measured). (Lower panel) Allicin-treated cells. (B) Immunoblot analysis of extracts (20 μg protein/lane) from allicin treated HL60 cells at various time of allicin (5 μM) treatment. The degrees of cytochrome *c* release into the cytosol and of caspase 9 and caspase 3 activation were assessed. β-Actin served as a control to the amount of loaded protein. The analysis of caspase 3, 9 and β-actin was done on the same blot after stripping. The data were obtained from one representative experiment (total of three independent experiments). (C) Staining of HL60 cells with MitoTracker Red CMXRos. HL60 cells treated with allicin (5 μM, 6 h) were collected, resuspended in fresh medium and were stained for 30 min with MitoTracker Red CMXRos (0.05 μM, 30 min). After washing twice with PBS, cells were examined by fluorescence microscopy (original magnification ×40).

level after 18 h. The band of cleaved caspase 9 appeared at 24 h, reached a maximal intensity at 48 h and was still seen at 72 h. Cleaved caspase 3 appeared at 30 h, became intense at 48 h and did not fade after 72 h (data not shown). Cleaved caspase 8 was not observed in either cell line after allicin treatment (data not shown).

3.2.4. Impaired mitochondrial activity

Mitochondrial activity was monitored with the XTT assay in cells treated with allicin (5 and 20 μM for HL60 and U937, respectively) for 16 h (Fig. 4). Both cell lines behaved similarly, showing a residual mitochondrial activity 65±5% in HL60 and 62±5% in U937 cells. At

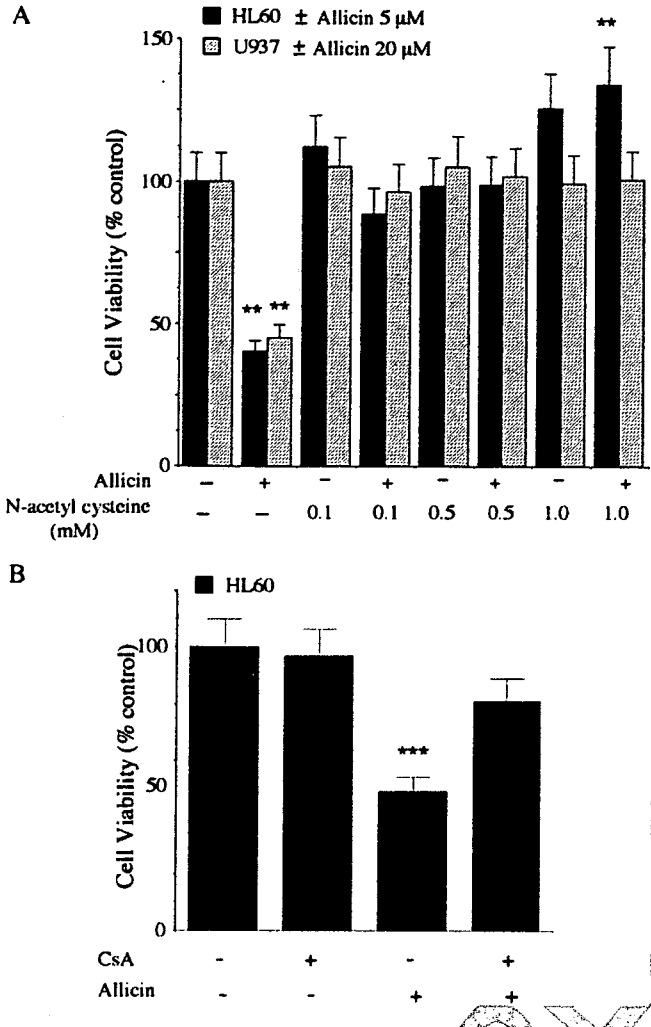

Fig. 4. (A) Allicin effect on cell viability in the absence or presence of *N*-acetyl cysteine. HL60 and U937 cells (100,000 cells/ml) were treated with allicin (5 or 20 μM, respectively) for 16 h, in the absence or presence of *N*-acetyl cysteine at 0.1, 0.5 and 1.0 mM. Cell viability was measured by the XTT assay after 3 h of incubation at 37°C with 5% CO_2. Means±S.D. of one experiment (n=6) are shown (total of three independent experiments). **P<01 represents a significant difference from nontreated cells, based on one-way ANOVA followed by Dunnett's test. (B) Allicin effect on HL60 cell viability following a 1-h CsA (5 μM) pretreatment. HL60 cells (100,000 cells/ml) were treated with or without allicin (5 μM) for 16 h. Cell viability was measured by the XTT assay. Means±S.D. of one experiment (n=6) are shown (total of three independent experiments). ***P<001, represents significant difference compared with nontreated cells by one-way ANOVA followed by Bonferroni's multiple comparison test.

this stage, the drop in mitochondrial activity was not accompanied by a significant change in cell number. Such a change was observed only after 24 h. Nontreated HL60 cells proliferated at a higher rate than nontreated U937 cells. Although after 24 h nontreated HL60 cells exceeded nontreated U937 cells in number, mitochondrial activity (measured by XTT assay) in U937 cells (0.869±0.025 OD units at 450 nm, n=6) was significantly higher than that in HL60 cells (0.498±0.073 OD units, n=6) (P<001). These results indicate a higher battery of mitochondrial enzymes in U937 cells and suggest a higher resistance to allicin. When cells were treated with allicin in the presence of NAC (0.1–1.0 mM), mitochondrial metabolic activity was not impaired, and the antiproliferative effect of allicin was precluded (Fig. 4A).

3.3. Allicin induces changes in mitochondrial membrane potential

Nontreated cells showed strong staining with MitoTracker Red CMXRos, indicating the negative membrane potential of the mitochondria and the accumulation of the lipophilic dye. In HL60 cells treated with allicin (5 μM, 6 h the staining intensity decreased significantly, indicating changes in the mitochondrial membrane potential (Fig. 3C). Reduced mitochondrial staining in allicin-treated (20 μM) U937 cells occurred much slower; changes were observed 24 h after treatment, and the decline continued up to 40 h (data not shown).

A deeper insight into the involvement of mitochondrial permeability transition pore (mPTP) in the cytotoxicity of allicin was gained by using cyclosporine A (CsA), an inhibitor of adeninenucleotide translocator. HL60 cells were preincubated with 5 μM CsA forl h and then treated with allicin for 16 or 20 h. CsA inhibited the detrimental effects of allicin on cell viability as determined by the XTT assay (~80% residual viability for CsA pretreatment; ~50% for allicin alone). There was no significant difference between nontreated and CsA-treated cells (P>.05). No significant difference was found between CsA alone and CsA followed by allicin treated cells (P>.05) (Fig. 4B). CsA-pretreated cells were stained with Hoechst 33342 and MitoTracker Red CMXRos. CsA pretreatment prevented the nuclear condensation induced by treatment with allicin alone (Fig. 5). Mitochondrial staining also showed the preventive effect of CsA, whereby allicin-induced mitochondrial membrane depolarization was inhibited.

FACS analysis of HL60 cells treated with allicin (5 μM, 20 h) showed that 35.0% of the cells were apoptotic, whereas CsA pretreatment reduced the apoptotic fraction to 17.1% (P<05). Cell arrest at G2 was increased in allicin-treated cells with or without CsA pretreatment — 34.9% and 59.0%, respectively (Fig. 6). The fraction of HL60 cells at the G2 stage was 17.3% for nontreated cells and 18.9% for cells treated with CsA only (the difference is not significant).

3.4. Differences in GSH levels between HL60 and U937

GSH concentrations (nmol/total cell volume) in nontreated HL60 and U937 cells were almost the same: 3.4±0.48 mM and 3.7±0.55 mM, respectively. However, due to the differences in cell size between the two cell lines, analysis of GSH concentration expressed as a function of protein levels or cell numbers was also used. This analysis revealed significant differences between the GSH concentrations in the two cell lines. In nontreated HL60 cells, GSH concentration was 20.94±3.15 nmol/mg protein, and in nontreated U937 cells, 30.80±6.04 nmol/mg protein (P<02). The

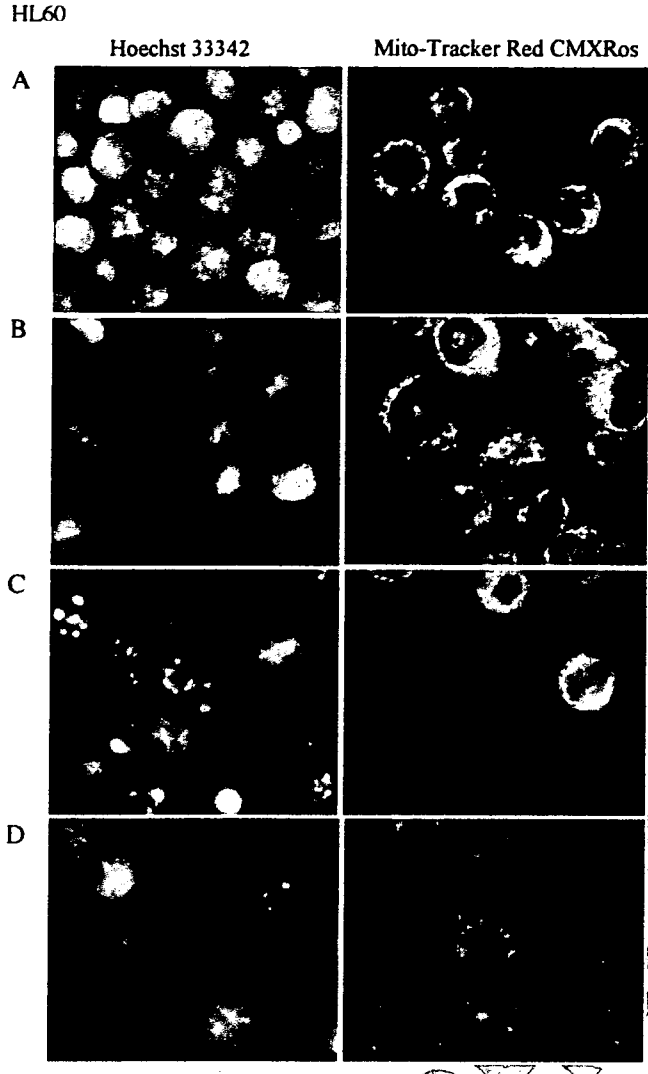

Fig. 5. Morphological effects of allicin on CsA pretreated HL60 cells. Cells (200,000 cells/ml) with or without CsA pretreatment (5 μM, 1h) were diluted and incubated in the presence or absence of allicin (5 μM) for 16 h. Cells were stained with Hoechst 33342 (5 μg/ml) or with Mito-Tracker Red CMXRos (50 nM) for 30 min. Cells were washed twice with PBS and examined by fluorescence microscopy. (A) HL60 nontreated. (B) CsA-treated. (C) Allicin-treated. (D) CsA- and allicin-treated.

difference was found to be even higher when cell numbers were considered, GSH concentration in HL60 cells was 3.7±0.56 nmol/10^6 cells whereas, in U937 cells, approximately twice as much [7.7±1.08 nmol/10^6 cells (P<001)].

3.5. Allicin-induced GSH depletion

Allicin treatment of HL60 cells caused a rapid decrease in GSH concentration, reaching its lowest point at about 30 min. A spontaneous recovery occurred, reaching the basal level of GSH (Fig. 7A). The highest GSH levels were observed in HL60 cells between 2–24 h after adding allicin. In allicin-treated U937 cells, a decrease in GSH levels to a minimal value occurred 2–4 h after treatment, and it was followed by a gradual increase to the basal GSH level (Fig. 7B).

3.6. Allicin-induced GSH depletion in the cells pretreated with BSO

In HL60 cells treated with BSO, an inhibitor of γ-glutamyl-cysteine synthetase (GGCS) (0.4 mM, 20 h) GSH levels decreased to 1.45±0.25 nmol/10^6 cells. No cell death was observed, but there was a slight decrease in the proliferation rate (×1.7 after 20 h as compared to ×2.1 in

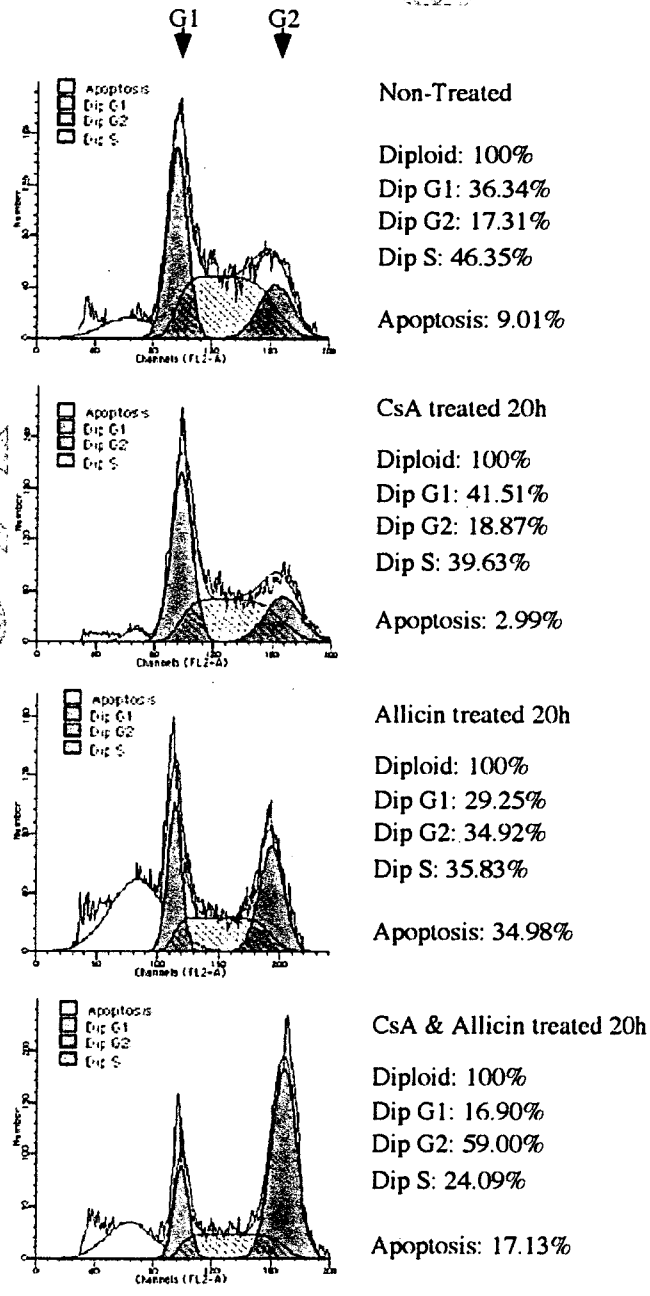

Fig. 6. Cell cycle analysis of allicin-treated HL60 cells. Cells (200,000 cells/ml, 1.5×10^6) with or without CsA pretreatment (5 μM, 1 h) were diluted and incubated in absence or presence of allicin (5 μM) for 20 h. The cells were stained with propidium iodide in the presence of RNase A and Triton X-100, as described in Materials and methods. The data represent one experiment (total of three independent experiments).

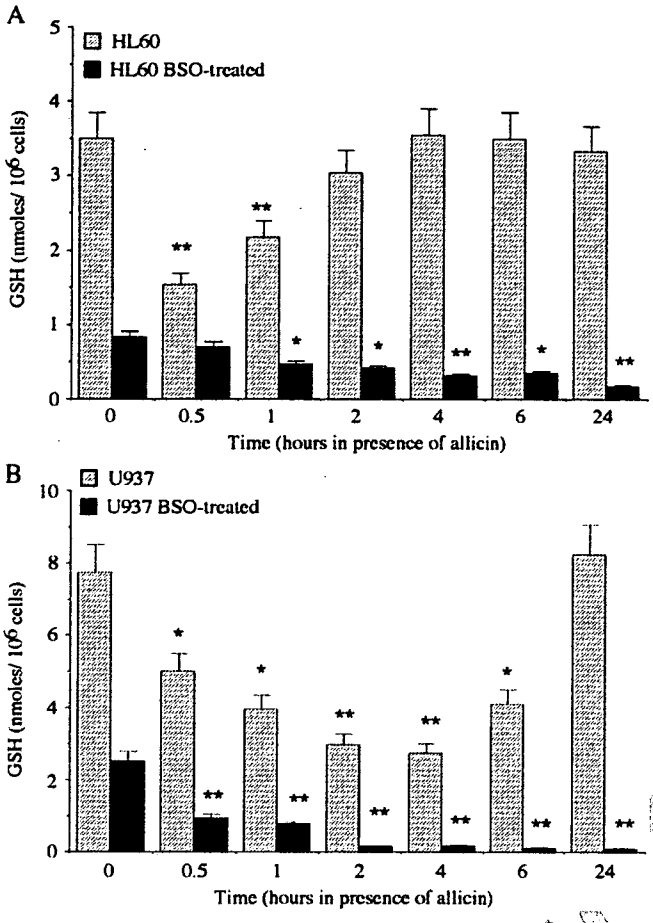

Fig. 7. Time-dependent decrease of GSH levels in allicin-treated HL60 and U937 cells after BSO pretreatment. Cells were pretreated with or without 0.4 mM BSO for 20h. HL60 and U937 cell cultures were diluted to 100,000 cells/ml and were grown in the presence of allicin (5 and 20 μM, respectively). At each time point, 30-ml samples were harvested and washed twice with PBS. Cell pellets were extracted with 5% metaphosphoric acid and analyzed for GSH content and protein concentration. Means±S.D. of one representative experiment (total of three independent experiments).

nontreated cells). Allicin (5 μM) applied to HL60 cells pretreated with BSO (0.4 mM, 20 h) caused an additional GSH decrease to 0.65±0.13 nmol/10^6 cells after 1 h (Fig. 7A, black column). There was no recovery of GSH as in the case of HL60 cells treated with allicin alone. In U937 cells pretreated with BSO (0.4 mM, 20 h), GSH levels decreased to 1.06±0.14 nmol/10^6 cells. Also, in this case, no cell death was observed and cells were still proliferating. When BSO-pretreated U937 cells were incubated with allicin (20 μM), GSH levels further decreased to 0.33±0.08 nmol/10^6 cells within 2 h (Fig. 7B, black column). A high rate of cell death (60–80%) occurred in both cell lines 24 h after allicin was applied to the culture.

3.7. Reduction potential in allicin-treated cells

Since allicin-treated cells lost their spherical structure and their volume could not be calculated from diameter measurement, we had to use another parameter to calculate changes in the intracellular reducing state resulting from fluctuations in 2GSH/GSSG ratios. Based on the assumption that 1-mg cell pellet is equivalent to 1 μl of volume, cell pellets were weighed, and GSH molar concentration was calculated accordingly (GSH amount/cell weight). Therefore, calculated reduction potential represents only approximate values. The intracellular pH of HL60 cells is 7.0 [37], and the reported E_0 for this pH is −240 mV [27]. Using the above E_0 values, reducing potential (E_{GSH}) calculated for nontreated HL60 was −207 mV (GSH 3.42±0.18 mM, GSSG 0.15±0.023 mM) and for allicin-treated (0.5 h) −169 mV (GSH 1.4±0.17 mM, GSSG 0.46±0.082 mM). The intracellular pH of U937 cells is 7.04 [38] or 7.2 [39], and the

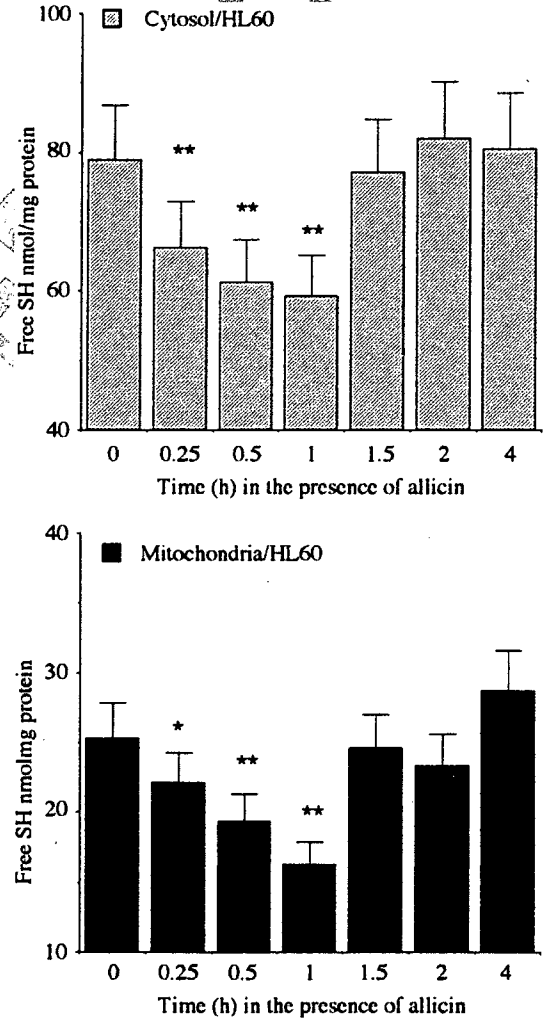

Fig. 8. Free SH contents in cytosolic and crude mitochondrial fractions from allicin-treated HL60 cells. Allicin (5 μM) was added to cells growing at density of 100,000 cells/ml. At various intervals, 100-ml samples were harvested at 4°C, washed twice with PBS and stored at −80°C overnight. Cell fractionation was done as described in Materials and methods. Total free SH and protein concentrations were determined as described in Materials and methods. The SH content at various time intervals in the cytosol (upper panel) and in the crude mitochondrial fraction (lower panel) are shown. Means±S.D. of one representative experiment (total of three independent experiments) [40].

reported E_0 values are −240 mV or −252 mV, respectively. The calculated reducing potential values of nontreated U937 cells were −206 mV or −218 mV (GSH 3.7±0.21 mM, GSSG 0.18±0.040 mM), and for allicin-treated cells (2 h), −173 mV or −185 mV (GSH 1.54±0.042 mM, GSSG 0.41±0.021 mM). The values obtained for nontreated cells are characteristic of cells in proliferation/differentiation state, whereas those obtained after allicin treatment are typically obtained in the apoptotic state.

3.8. Free SH in the cytosolic and mitochondrial fractions of HL60 cells

Total free SH concentrations were determined in the cytosol and in the crude mitochondrial fractions prepared from allicin-treated HL60 cells. The decrease in free SH in the cytosol (Fig. 8, upper panel) was accompanied by a decrease of free SH in the mitochondria (Fig. 8, lower panel). Since mitochondrial GSH is supplied from the cytoplasm and upon allicin treatment it was depleted in both cellular compartments, it was followed by a substantial decrease in the cell-reducing potential. Consequently, depolarization of the mitochondrial membrane occurred and triggered a chain of apoptotic events leading to cell death.

4. Discussion

GSH, cysteine and accessible free SH groups of various proteins and peptides are rapidly oxidized by allicin to their respective allyl-SS derivatives [19,22]. The mixed disulfide formed is less active than allicin, yet it can easily react with free SH in thiol-disulfide exchange reactions, and produce, at the end of a series of reactions, the oxidized form of glutathione (GSSG), the oxidized form of cysteine (cystine) and glutathiolated S proteins. The leaving group (allyl-mercaptan) is volatile and rapidly disappears.

Glutathione is the major regulator of the thiol-disulfide redox state of living cells (reviewed in Refs. [29,41–43]). Alterations in cellular free thiols have already been described as a key event in the generation of apoptosis (reviewed in [44,45]).

In this study, allicin induced mitochondrial release of cytochrome *c*, activation of caspase 9 and 3 and DNA fragmentation in HL60 and U937 cell lines in a concentration- and time-dependent manner. GSH depletion had been shown to be associated with cell surface blebbing in hepatocytes [46]. Here, cell blebbing occurred in both HL60 and U937 cells treated with allicin. The rate of free SH depletion from the cytosol and the mitochondria was similar, indicating that allicin penetrated the mitochondria and the cell membrane equally well and reacted with free SH in both compartments. Allicin induced an initial drop in GSH levels that was followed by a regeneration process, occurring several hours after treatment. This may be due to decreased feedback inhibition of GSH biosynthetic enzymes such as GGCS by GSH [45]. Conversely, in BSO-pretreated cells, there was no recovery of GSH after its allicin-induced depletion, as BSO is a direct inhibitor of GGCS. BSO pretreatment in allicin-treated U937 cells shortened the life span from 72 to 20 h, indicating that preliminary GSH depletion renders cells more sensitive to apoptosis. BSO-depleted GSH levels in U937 cells were, at this stage, similar to the inherent GSH level in HL60 cells and, hence, a similar degree of sensitivity to allicin.

Here, we have shown that allicin causes GSH depletion concomitantly in the cytosol and the mitochondria in HL60 cells. It is known that active GSH uptake by intact mitochondria occurs even at very low cytosolic GSH levels and that the rate of mitochondrial GSH depletion is much slower than that of the cytosol [47]. These are indications that mitochondria have more than one control mechanism to maintain GSH levels. Since BSO-induced depletion of GSH levels caused neither mitochondrial permeability transition nor apoptosis, it is likely that BSO treatment depletes GSH mainly from the cytosol, whereas allicin induced depletion of mitochondrial GSH trigger the apoptotic process. Moreover, CsA (mPTP inhibitor) pretreatment of HL60 cells inhibits allicin-induced mitochondrial permeability transition and cell death, corroborating the central role of mitochondria in the apoptotic process induced by allicin. Simultaneous addition of NAC and allicin to cells provided protection against the apoptotic damage. NAC sequestered the harmful activity by competing with GSH for the reaction with allicin.

The following allicin-induced apoptotic scenario can be deduced from this study: Allicin penetrates the cells and readily reacts with any exposed SH present in its vicinity. As GSH is the most abundant thiol molecule in the cytosol and the mitochondria, it is the main target for allicin reaction. The reaction with glutathione leads to an immediate change in the ratio GSH/GSSG. The increased concentration of GSSG and the depletion of GSH brings about a decrease in the cellular reduction potential state. Concomitantly, mitochondrial damage occurs, as is evident from changes in membrane potential, its decreased enzymatic activity and the release of cytochrome *c* to the cytosol. Upon its release, cytochrome *c* participates in the activation of the caspase 9, followed by activation of caspase 3.

Allicin induced cell cycle arrest at G2/M in HL60 cells (~35%). Upon CsA pretreatment, the percentage of cells at G2/M was even higher (~59%). After pretreatment of HL60 cells with CsA and 40-h incubation with allicin, there was no change in the number of viable cells, neither were there signs of cell breakage. By using CsA, it could be shown that the effect of allicin on cell cycle arrest was independent of its proapoptotic activity. The mechanism by which allicin induces G2/M cell arrest is not clear, but a clue may reside in its ability to inhibit microtubule assembly. It had been shown that microtubule assembly is disrupted by direct modification of tubulin SH groups [48–50] and that adding GSH to an in vitro microtubule assembly system disrupted by SH modification restores tubulin polymerization [51].

Here we have shown that, in allicin-treated cells, there is an increase in GSH synthesis. Therefore, cell cycle arrest would be expected to expire after tubulin recovery. However, the protracted G2/M phase induced by cyclosporine A and allicin suggests an additional modification of a critical pathway that needs an extended period to regenerate.

Allicin disappears from the medium very rapidly due to its penetration into the cells and its reaction with SH group. When applied to HL60 cells (5 $\mu M/10^5$ cells/ml) or to U937 cells (20 $\mu M/10^5$ cells/ml), it could not be detected in the medium after 2 h or 6–8 h in HL60 or U937 cells, respectively. The consumption of allicin within such a short time enables full activity of SH-dependent apoptotic enzymes such as the cysteine proteases and caspases 9 and 3 [52].

Cell sensitivity to allicin was shown to be dependent on the intracellular content of GSH. Since there is a significant difference in cell size between the two cell lines examined, comparing GSH amount/cell number showed that HL60 cells contained 3.7 nmol GSH/10^6 cells, whereas U937 cells contained 7.7 nmol GSH/10^6 cells. The differences in GSH intracellular content reflect differences in sensitivity to allicin. The higher the GSH, the less sensitive to allicin cells are, and the slower the apoptotic signs appear.

The allicin-induced decrease in GSH levels modulates the redox state of cells. In allicin-treated HL60 cells, the ratio of [GSH]/[GSSG or GSSA] changed within the first 30 min and the reducing potential reached −170 mV, whereas in U937 cells, it took 2 h to reach the same level. Such a high value is typical of the apoptotic state [27].

Since GSSA (the first main product of allicin reaction with GSH) is able to prevent the formation of free radicals [19], it is likely that the initial event inducing apoptosis does not occur via the generation of reactive oxygen species but rather through mitochondrial membrane depolarization or through a more finely tuned event mediated by protein modification upon creating a mixed disulfide [19,53]. Oxidative stress incurred by the accumulation of peroxides is a secondary event probably happening after the short-lived GSSA is eliminated from the cells.

It was reported that, in BSO-treated U937 cells, the depletion of GSH and the release of cytochrome *c* into the cytosol were counteracted by cell-repair systems involving nuclear factor κB and heat shock proteins [54]. Our results show that CsA and NAC prevented apoptosis induced by allicin. Taken together, the role allicin plays may be through direct modification of specific free SH in proteins, such as reside in apoptotic repair system, in the mPTP [55] or others.

Acknowledgement

We would like to thank Dr. A. Gross, Department of Biological Regulation, Weizmann Institute of Science for critical reading of the manuscript, and Mrs. Anna Gakamsky for her help in the statistical analysis.

References

[1] Stoll A, Seebeck E. Chemical investigation on alliin, the specific principle of garlic. Adv Enzymol 1951;11:377–400.

[2] Koch HP, Lawson LD. Garlic: the Science and therapeutic application of *Allium sativum* L. and related species2nd ed. 1996 [Baltimore].

[3] Elkayam A, Mirelman D, Peleg E, Wilchek M, Miron T, Rabinkov A, et al. The effects of allicin and enalapril in fructose-induced hyperinsulinemic hyperlipidemic hypertensive rats. Am J Hypertens 2001;14:377–81.

[4] Eilat S, Oestraicher Y, Rabinkov A, Ohad D, Mirelman D, Battler A, et al. Alteration of lipid profile in hyperlipidemic rabbits by allicin, an active constituent of garlic. Coron Artery Dis 1995;6:985–90.

[5] Abramovitz D, Gavri S, Harats D, Levkovitz H, Mirelman D, Miron T, et al. Allicin-induced decrease in formation of fatty streaks (atherosclerosis) in mice fed a cholesterol-rich diet. Coron Artery Dis 1999; 10:515–9.

[6] Gonen A, Harats D, Rabinkov A, Miron T, Mirelman D, Wilchek M, et al. The antiatherogenic effect of allicin: possible mode of action. Pathobiology 2005;72:325–34.

[7] Lang A, Lahav M, Sakhnini E, Barshack I, Fidder HH, Avidan B, et al. Allicin inhibits spontaneous and TNF-alpha induced secretion of proinflammatory cytokines and chemokines from intestinal epithelial cells. Clin Nutr 2004;23:1199–208.

[8] Agarwal KC. Therapeutic actions of garlic constituents. Med Res Rev 1996;16:111–24.

[9] Hirsch K, Danilenko M, Giat J, Miron T, Rabinkov A, Wilchek M, et al. Effect of purified allicin, the major ingredient of freshly crushed garlic, on cancer cell proliferation. Nutr Cancer 2000;38:245–54.

[10] Knowles LM, Milner JA. Possible mechanism by which allyl sulfides suppress neoplastic cell proliferation. J Nutr 2001;131:1061S–6S.

[11] Sun L, Wang X. Effects of allicin on both telomerase activity and apoptosis in gastric cancer SGC-7901 cells. World J Gastroenterol 2003;9:1930–4.

[12] Oommen S, Anto RJ, Srinivas G, Karunagaran D. Allicin (from garlic) induces caspase-mediated apoptosis in cancer cells. Eur J Pharmacol 2004;485:97–103.

[13] Park SY, Cho SJ, Kwon HC, Lee KR, Rhee DK, Pyo S. Caspase-independent cell death by allicin in human epithelial carcinoma cells: involvement of PKA. Cancer Lett 2005;224:123–32.

[14] Antlsperger DSM, Dirsch VM, Ferreira D, Su JL, Kuo ML, Vollmar AM. Ajoene-induced cell death in human promyeloleukemic cells does not require JNK but is amplified by the inhibition of ERK. Oncogene 2003;22:582–9.

[15] Jin Z, El-Deiry WS. Overview of cell death signaling pathways. Cancer Biol Ther 2005;4:139–63.

[16] Hsu YT, Wolter KG, Youle RJ. Cytosol-to-membrane redistribution of Bax and Bcl-X1 during apoptosis. Proc Natl Acad Sci U S A 1997;94:3668–72.

[17] Wolter KG, Hsu YT, Smith A, Nechushtan A, Xi X, Youle RJ. Movement of Bax from the cytosol to mitochondria during apoptosis. J Cell Biol 1997;139:1281–92.

[18] Miron T, Rabinkov A, Mirelman D, Wilchek M, Weiner L. The mode of action of allicin: its ready permeability through phospholipid membranes may contribute to its biological activity. Biochim Biophys Acta 2000;1463:20–30.

[19] Rabinkov A, Miron T, Mirelman D, Wilchek M, Glozman S, Yavin E, et al. *S*-allylmercaptoglutathione: the reaction product of allicin with glutathione possesses SH-modifying and antioxidant properties. Biochim Biophys Acta 2000;1499:144–53.

[20] Xiao H, Parkin KL. Antioxidant functions of selected allium thiosulfinates and *S*-alk(en)yl-L-cysteine sulfoxides. J Agric Food Chem 2002;50:2488–93.

[21] Okada Y, Tanaka K, Sato E, Okajima H. Kinetic and mechanistic studies of allicin as an antioxidant. Org Biomol Chem 2006;4:4113–7.

[22] Rabinkov A, Miron T, Konstantinovski L, Wilchek M, Mirelman D, Weiner L. The mode of action of allicin: trapping of radicals and

interaction with thiol containing proteins. Biochim Biophys Acta 1998;1379:233–44.
[23] Freeman F, Kodera Y. Garlic chemistry-stability of *S*-(2-propenyl) 2-propene-1-sulfinothioate (allicin) in blood, solvents, and simulated physiological fluids. J Agric Food Chem 1995;43:2332–8.
[24] Lachmann G, Lorenz D, Radeck W, Steiper M. The pharmacokinetics of the S35 labeled garlic constituents alliin, allicin and vinyldithiine. Arzneimittelforschung 1994;44:734–43.
[25] Miron T, Mironchik M, Mirelman D, Wilchek M, Rabinkov A. Inhibition of tumor growth by a novel approach: in situ allicin generation using targeted alliinase delivery. Mol Cancer Ther 2003; 2:1295–301.
[26] Arditti F, Rabinkov A, Miron T, Reisner Y, Berrebi A, Wilchek M, et al. Apoptotic killing of B-chronic lymphocytic leukemia tumor cells by allicin generated in situ using a rituximab–alliinase conjugate. Mol Cancer Ther 2005;4:325–31.
[27] Schafer FQ, Buettner GR. Redox environment of the cell as viewed through the redox state of the glutathione disulfide/glutathione couple. Free Radic Biol Med 2001;30:1191–212.
[28] Jonas CR, Ziegler TR, Gu LH, Jones DP. Extracellular thiol/disulfide redox state affects proliferation rate in a human colon carcinoma (Caco2) cell line. Free Radic Biol Med 2002;33:1499–506.
[29] Gilbert HF. Molecular and cellular aspects of thiol-disulfide exchange. Adv Enzymol Relat Areas Mol Biol 1990;63:69–172.
[30] Stoll A, Seebeck E. Allium compounds V. The synthesis of natural alliin and its three optical active isomers. Helv Chim Acta 1951;34: 481–7.
[31] Miron T, SivaRaman H, Rabinkov A, Mirelman D, Wilchek M. A method for continuous production of allicin using immobilized alliinase. Anal Biochem 2006;351:152–4.
[32] Nakagawa Y, Iinuma M, Matsuura N, Yi K, Naoi M, Nakayama T, et al. A potent apoptosis-inducing activity of a sesquiterpene lactone, arucanolide, in HL60 cells: a crucial role of apoptosis-inducing factor. J Pharmacol Sci 2005;97:242–52.
[33] Grinberg M, Schwarz M, Zaltsman Y, Eini T, Niv H, Pietrokovski S, et al. Mitochondrial carrier homolog 2 is a target of tBID in cells signaled to die by tumor necrosis factor alpha. Mol Cell Biol 2005;25: 4579–4590.
[34] Gornall A, Bardawill C, David M. Determination of serum proteins by means of the biuret reaction. J Biol Chem 1949;177:751–66.
[35] Anderson ME. Determination of glutathione and glutathione disulfide in biological samples. Methods Enzymol 1985;113:548–55.
[36] Riddles PW, Blakeley RL, Zerner B. Ellman's reagent: 5,5′-dithiobis (2-nitrobenzoic acid) — a reexamination. Anal Biochem 1979;94: 75–81.
[37] Restrepo D, Kozody DJ, Spinelli LJ, Knauf PA. pH Homeostasis in promyelocytic leukemic HL60 cells. J Gen Physiol 1988;92:489–507.
[38] Oehler R, Zellner M, Hefel B, Weingartmann G, Spittler A, Struse HM, et al. Influence of heat shock on cell volume regulation: protection from hypertonic challenge in a human monocyte cell line. FASEB J 1998;12:553–60.
[39] Nilsson C, Kagedal K, Johansson U, Ollinger K. Analysis of cytosolic and lysosomal pH in apoptotic cells by flow cytometry. Methods Cell Sci 2003;25:185–94.
[40] Amonkar SV, Reeves EL. Mosquito control with active principle of garlic, *Allium sativum*. J Econ Entomol 1970;63:1172–5.
[41] Powis G. Anticancer drugs acting against signaling pathways. Curr Opin Oncol 1995;7:554–9.
[42] Sies H. Glutathione and its role in cellular functions. Free Radic Biol Med 1999;27:16–21.
[43] Moran LK, Gutteridge JM, Quinlan GJ. Thiols in cellular redox signalling and control. Curr Med Chem 2001;8:763–72.
[44] Meister A. Glutathione metabolism. Methods Enzymol 1995;251:3–7.
[45] Lash LH. Mitochondrial glutathione transport: physiological, pathological and toxicological implications. Chem Biol Interact 2006;163: 54–67.
[46] Jewell SA, Bellomo G, Thor H, Orrenius S, Smith M. Bleb formation in hepatocytes during drug metabolism is caused by disturbances in thiol and calcium ion homeostasis. Science 1982;217:1257–9.
[47] Meister A. Mitochondrial changes associated with glutathione deficiency. Biochim Biophys Acta 1995;1271:35–42.
[48] Kuriyama R, Sakai H. Role of tubulin-SH groups in polymerization to microtubules. Functional-SH groups in tubulin for polymerization. J Biochem (Tokyo) 1974;76:651–4.
[49] Li M, Ciu JR, Ye Y, Min JM, Zhang LH, Wang K, et al. Antitumor activity of Z-ajoene, a natural compound purified from garlic: antimitotic and microtubule-interaction properties. Carcinogenesis 2002;23:573–9.
[50] Xiao D, Pinto JT, Soh JW, Deguchi A, Gundersen GG, Palazzo AF, et al. Induction of apoptosis by the garlic-derived compound *S*-allylmercaptocysteine (SAMC) is associated with microtubule depolymerization and c-Jun NH(2)-terminal kinase 1 activation. Cancer Res 2003;63:6825–37.
[51] Nishida E, Kobayashi T. Relationship between tubulin SH groups and bound guanine nucleotides. J Biochem (Tokyo) 1977;81:343–7.
[52] Thornberry NA. Caspases: key mediators of apoptosis. Chem Biol 1998;5:R97–R103.
[53] Patya M, Zahalka MA, Vanichkin A, Rabinkov A, Miron T, Mirelman D, et al. Allicin stimulates lymphocytes and elicits an antitumor effect: a possible role of p21(ras). Int Immunol 2004;16:275–81.
[54] Filomeni G, Aquilano K, Rotilio G, Ciriolo MR. Antiapoptotic response to induced GSH depletion: involvement of heat shock proteins and NF-kappaB activation. Antioxid Redox Signal 2005; 7:446–55.
[55] McStay GP, Clarke SJ, Halestrap AP. Role of critical thiol groups on the matrix surface of the adenine nucleotide translocase in the mechanism of the mitochondrial permeability transition pore. Biochem J 2002541;367:548.

Apoptosis (2007) 12:835–840
DOI 10.1007/s10495-006-0525-7

Role of the mitochondrial membrane permeability transition in cell death

Yoshihide Tsujimoto · Shigeomi Shimizu

Published online: 21 November 2006

Abstract In recent years, the role of the mitochondria in both apoptotic and necrotic cell death has received considerable attention. An increase of mitochondrial membrane permeability is one of the key events in apoptotic or necrotic death, although the details of the mechanism involved remain to be elucidated. The mitochondrial membrane permeability transition (MPT) is a Ca^{2+}-dependent increase of mitochondrial membrane permeability that leads to loss of $\Delta\psi$, mitochondrial swelling, and rupture of the outer mitochondrial membrane. The MPT is thought to occur after the opening of a channel that is known as the permeability transition pore (PTP), which putatively consists of the voltage-dependent anion channel (VDAC), the adenine nucleotide translocator (ANT), cyclophilin D (Cyp D: a mitochondrial peptidyl prolyl-*cis*, *trans*-isomerase), and other molecule(s). Recently, significant progress has been made by studies performed with mice lacking Cyp D at several laboratories, which have convincingly demonstrated that Cyp D is essential for the MPT to occur and that the Cyp D-dependent MPT regulates some forms of necrotic, but not apoptotic, cell death. Cyp D-deficient mice have also been used to show that the Cyp D-dependent MPT plays a crucial role in ischemia/reperfusion injury. The anti-apoptotic proteins Bcl-2 and Bcl-x_L have the ability to block the MPT, and can therefore block MPT-dependent necrosis in addition to their well-established ability to inhibit apoptosis.

Y. Tsujimoto (✉) · S. Shimizu
Osaka University Medical School, Department of Medical Genetics, SORST of the Japan Science and Technology Agency, 2-2 Yamadaoka, Suita, Osaka 565-0871, Japan

Keywords Apoptosis · Necrosis · Mitochondria · Cyclophilin D · Cyclosporin A · Membrane permeability transition · Cytochrome c · Ischemia

Introduction

Apoptosis is a form of programmed cell death and an outline of the relevant signaling pathways at the molecular level is now well established. Mammalian cells possess two major apoptotic signaling pathways, which are known as the intrinsic pathway and the extrinsic pathway [1]. The intrinsic pathway involves an increase of outer mitochondrial membrane permeability that leads to the release of various proteins from the intermembrane space into the cytoplasm, including apoptogenic molecules such as cytochrome *c*, Smac/Diablo, HtrA2 (Omi), AIF, and DNaseG [1, 2]. In the presence of ATP (dATP), cytochrome *c* binds to Apaf-1 and triggers its oligomerization, after which pro-caspase-9 is recruited and undergoes autoactivation. The protein complex comprising cytochrome *c*, Apaf-1, and caspase-9 is called the "apoptosome". In short, an increase of outer mitochondrial membrane permeability is central to apoptosis [3, 4], and mitochondrial membrane permeability is directly regulated by the Bcl-2 family of proteins [4, 5] (see Fig. 1). However, the detailed mechanisms underlying the increase of outer mitochondrial membrane permeability during apoptosis and how this process is controlled by Bc1-2 family members are still to be determined. The model that was initially developed to explain the apoptotic increase of mitochondrial membrane permeability was based on the "mitochondrial membrane permeability transition" (MPT) [6], an event which has been appreciated for some time among investigators studying the mitochondria. This review summarizes recent progress with

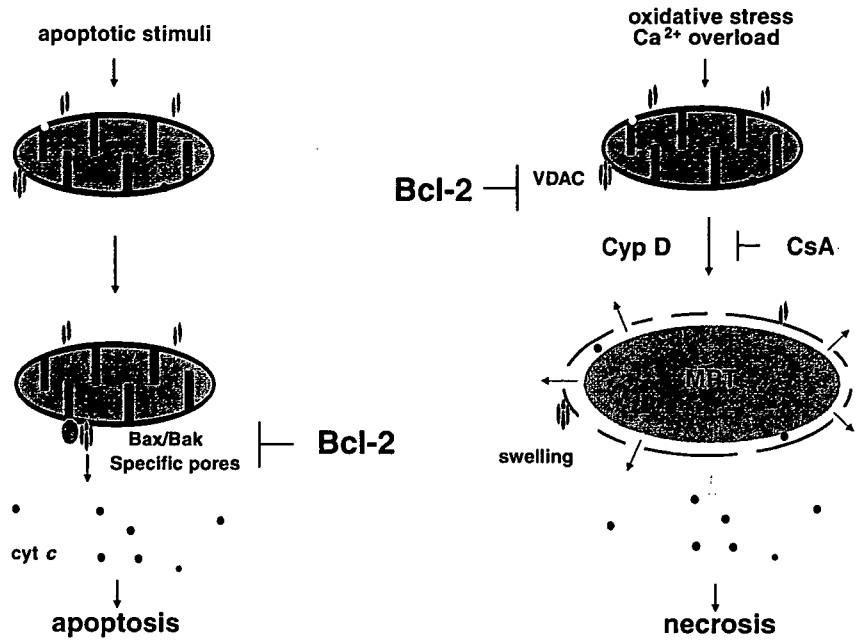

Fig. 1 Role of the mitochondria in apoptosis and necrosis. An increase in the permeability of the outer mitochondrial membrane is crucial for apoptosis to occur and is regulated by multidomain pro-apoptotic members of the Bcl-2 family (Bax and Bak), resulting in the release of several apoptogenic factors into the cytoplasm. In contrast, the Cyp D-dependent MPT involves an increase in the permeability of both the outer and inner mitochondrial membranes, and leads to necrosis induced by Ca^{2+} overload and oxidative stress. Both types of mitochondrial membrane permeability change are inhibited by anti-apoptotic members of the Bcl-2 family (Bcl-2 and Bcl-x_L)

regard to our understanding of the role of the MPT in cell death.

MPT

Mitochondria isolated from a variety of sources can show a sudden increase in the permeability of the inner mitochondrial membrane to solutes with a molecular mass of less than 1,500 Da, which results in the loss of $\Delta\psi$, mitochondrial swelling, and rupture of the outer mitochondrial membrane [7, 8] (see Fig. 1). This process is called the mitochondrial membrane permeability transition (MPT). The MPT can be induced under various conditions, such as exposure of mitochondria to Ca^{2+} together with inorganic phosphate. Although the molecular mechanisms of the MPT are largely unknown, the most widely accepted model (working hypothesis) is that it occurs after the opening of a channel complex that has been termed the permeability transition pore (PTP), which is thought to consist of the voltage-dependent anion channel (VDAC: outer membrane channel), the adenine nucleotide translocator (ANT: inner membrane channel), cyclophilin D (Cyp D), and possibly other molecule(s) [9] (see Fig. 2). However, it still remains uncertain whether the PTP really exists and what its exact nature is. Moreover, several experimental findings are difficult to explain by this model (see the introduction of [10]). A role of the ANT in the MPT is supported by MPT inhibition and activation by bonkrekic acid and atractyloside, respectively, which are ANT ligands [11]. Cyp D is a mitochondrial member of the cyclophilin family, which possesses peptidyl prolyl-*cis*, *trans*-isomerase (PPIase) activity and has a crucial role in protein folding [12]. The putative role of Cyp D in regulating the MPT is based on the observation that cyclosporin A (CsA), a specific inhibitor of the cyclophilin family, blocks the MPT [13]. Since CsA inhibits PPIase and the MPT at similar concentrations, PPIase activity may be critical for the MPT to occur. Cyp D resides in the mitochondrial matrix, but becomes associated with the inner mitochondrial membrane during the MPT. Based on the enzymatic activity of Cyp D as a PPIase, it may induce a conformational change of an inner membrane channel such as the ANT that leads to an increase of inner membrane permeability. In addition to the CsA-sensitive and Ca^{2+}-dependent ("regulated") MPT, the existence of a CsA-insensitive ("unregulated") MPT has also been suggested, although its mechanism and relationship to the CsA-sensitive MPT are totally unknown [10].

In the mid-1990s, the MPT attracted the attention of investigators in the cell death field, because it was reported that at least some forms of apoptosis could be inhibited by CsA, suggesting a role of the CsA-sensitive MPT in this process of cell death [9, 14]. A possible role of the MPT in apoptosis is also supported by the finding that apoptosis can sometimes be inhibited by bonkrekic acid [11, 15]. The CsA-sensitive MPT has also been implicated in remodeling of the mitochondrial cristae and mobilization of cytochrome *c* stores from the cristae during apoptosis, which promotes the complete release of cytochrome *c* [16]. However, the overall role of the MPT in apoptosis was still controversial, because there have been a number of reports that apoptosis

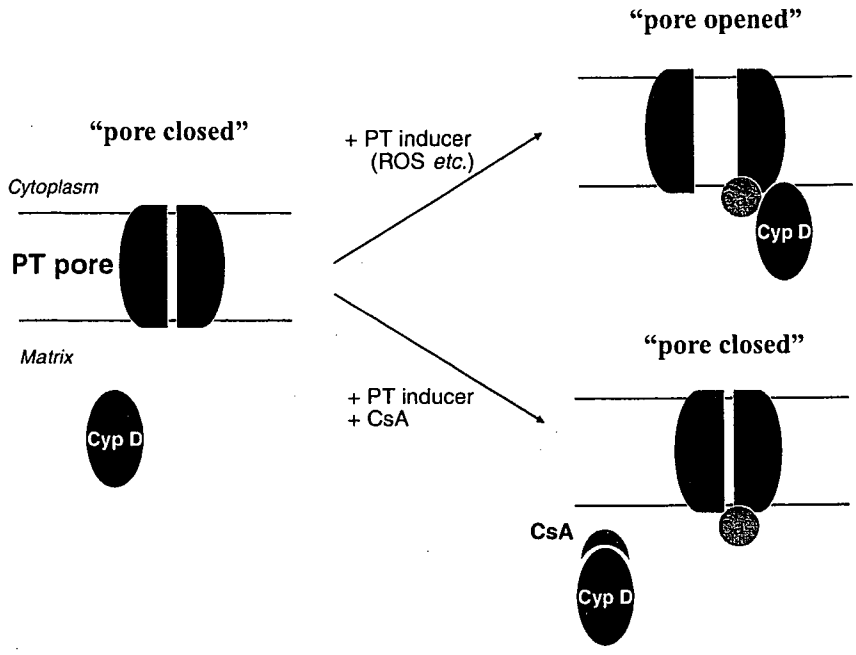

Fig. 2 Model of the MPT pore Under normal conditions, Cyp D is localized to the mitochondrial matrix, and the MPT pore is closed. In the presence of permeability transition inducers, Cyp D is considered to bind to and induce a conformational change of a channel in the inner membrane, resulting in opening of the MPT pore. Cyclosporin A (CsA) binds to and inhibits Cyp D to prevent MPT pore opening

is not inhibited by CsA [17]. Also, it has been demonstrated that $\Delta\psi$ occurs after cytochrome *c* release in at least some types of apoptosis, suggesting that the MPT is not always the trigger for cytochrome *c* release and cell death. This issue was recently been solved by studies performed in Cyp D-deficient mice, as discussed later.

Are the VDAC, the ANT, and Cyp D essential for the MPT?

It has long been thought that the VDAC, the ANT, and Cyp D play an essential role in the MPT, but convincing evidence was lacking until very recently.

An important role of the VDAC in the MPT has been supported by the following findings: (1) the electrophysiological properties of the PTP are strikingly similar to those of the VDAC incorporated in planar phospholipids bilayers [18, 19]; (2) various factors that alter VDAC channel properties, such as addition of NADH, Ca^{2+}, or glutamate, as well as binding to hexokinase II [20–24], also modulate PTP activity [25–27]; and (3) chromatography of mitochondrial extracts on a Cyp D affinity column leads to purification of the VDAC associated with the ANT [28].

The most convincing evidence about involvement of the VDAC in the MPT should theoretically be obtained by studies employing VDAC-deficient cells. Such a study was recently performed with mitochondria isolated from VDAC1-deficient cells, and it was found that VDAC1-deficient mitochondria still undergo the MPT normally, suggesting that VDAC1 is not important for this process. However, this result could have been due to compensation for VDAC1 deficiency by other isoforms, including VDAC2 and VDAC3. So far, experimental evidence for a direct role of the VDAC in the MPT has been provided by studies using specific anti-VDAC antibodies [29]. Two polyclonal anti-VDAC antibodies, which recognize different VDAC epitopes and inhibit its activity in liposomes [29], have been shown to inhibit the Ca^{2+}-induced MPT [29], supporting a crucial role for the VDAC in this process.

The ANTs (ANT1 and 2 in mice and ANT1, 2, and 3 in humans) are also considered to be important for the MPT. It has been demonstrated that Cyp D interacts directly with the ANT, although it is not known whether CsA inhibits this interaction [28, 30]. Regarding the role of the ANT in the MPT, considerable progress was made recently because it was shown that liver mitochondria from mice lacking both ANT1 and ANT2 still underwent the MPT, although the triggering Ca^{2+} concentration was slightly increased [31]. This finding suggests that ANT1/2 only play a limited role, if any, in the MPT or else that deficiency of ANT1/2 was compensated by other channel(s). The lack of an important role for the ANT in the MPT would be consistent with the observation that mitochondria isolated from yeast lacking the ANT still undergo MPT-like changes, including loss of membrane potential and swelling in response to ethanol, which are very similar events to those occurring in mammalian mitochondria during the MPT [32]. However, it is unknown whether

yeast mitochondria undergo a real MPT, because swelling of these mitochondria and loss of membrane potential in response to ethanol are not inhibited by CsA, although this inability of CsA to inhibit MPT-like events might be due to its inability to inhibit a Cyp D counterpart in yeast mitochondria. If the ANT is not involved in the MPT, the other channel(s) that are actually involved might be ANT-like inner membrane channels, because the MPT is modulated by ANT ligands such as bonkrekic acid or atractyloside and is accompanied by loss of $\Delta\psi$ (i.e., increased permeability of the inner mitochondrial membrane). Identification of one or more channels in the inner mitochondrial membrane that are directly involved in the MPT and might be targets of Cyp D would be an important step forward.

The role of Cyp D in the MPT was initially suggested by the finding that the MPT is blocked by CsA, which is known to inhibit the PPIase activity of cyclophilins. This finding has recently been confirmed by studies performed employing Cyp D gene (*ppif*)-deficient mice [33–36]. It has been demonstrated that Cyp D-deficient mitochondria isolated from the livers of these mice do not undergo the CsA-sensitive MPT in response to a variety of inducers, including Ca^{2+}, atractyloside, and H_2O_2. Because the MPT does not occur, these mitochondria accumulate a much higher concentration of Ca^{2+} than control mitochondria [33, 36]. However, the CsA-insensitive MPT (with loss of $\Delta\psi$ and swelling) can still occur when these Cyp D-deficient mitochondria are exposed to high concentrations of Ca^{2+} [33, 35]. In addition, Cyp D-deficient mitochondria show a normal response to reagents like ubiquinone and thiol oxidants that cause the CsA-insensitive MPT [35]. The CsA-sensitive MPT and CsA-insensitive MPT might share a common mechanism, because both forms of MPT are inhibited by ubiquinone 0 [35]. This finding might also suggest that Cyp D only sensitizes the mitochondria to the Ca^{2+}-induced MPT, although these two forms of MPT might be mediated by different mechanisms. This issue will only be solved by identification of the essential players involved in the MPT. In any case, it has been confirmed that Cyp D has a specific role in the CsA-sensitive MPT.

Although it is now clear that the Cyp D is an essential component of the CsA-sensitive MPT, there are still many questions to be answered. More studies are needed to elucidate the molecular nature of the MPT pore complex. Assuming that Cyp D interacts as a PPIase with other molecules essential for the MPT that probably reside in the inner mitochondrial membrane, a promising approach would be the isolation of a protein complex containing Cyp D and the VDAC. Another issue would be investigation of the relationship between the Cyp D-dependent MPT and the unregulated MPT. Furthermore, does the unregulated MPT have a role in apoptosis or other forms of cell death?

Role of the MPT

For a long time, it has been unclear whether the CsA-sensitive MPT plays an important role in the apoptotic increase of mitochondrial membrane permeability. However, studies of Cyp D-deficient mice have finally solved this issue. Various cells isolated from Cyp D-deficient mice, such as thymocytes, embryonic fibroblasts (MEFs), and hepatocytes, undergo apoptosis normally in response to various stimuli, including etoposide, stautosporine, and tumor necrosis factor-α [33–36]. Small intestinal cells from Cyp D-deficient mice are also as sensitive to X ray-induced apoptosis as cells from control mice [33]. These results provide the most compelling evidence that the CsA-sensitive MPT is not essential for apoptosis. Of course, it remains possible that some forms of apoptosis might be mediated by the CsA-sensitive MPT, and thus inhibited by CsA. However, the inhibitory effect of CsA on apoptosis might need to be more carefully evaluated because it is usually studied at relatively high CsA concentrations that could inhibit other targets, including cytoplasmic cyclophilins involved in transcriptional regulation, thus having a secondary effect on apoptosis. Accordingly, it may be necessary to re-evaluate CsA-dependent inhibition of apoptosis by using Cyp D-deficient cells or by silencing Cyp D to assess the real effect of CsA.

Several studies have indicated that overexpression of Cyp D protects cells against some forms of apoptosis. For example, the overexpression of CypD inhibits apoptosis induced by overexpression of caspase-8 (but not Bax) or by exposure to arsenic trioxide [37, 38]. It may be possible that these forms of apoptosis are mediated by the MPT, which is somehow affected by Cyp D overexpression. However, studies of transgenic mice with myocardial expression of Cyp D have revealed that cardiac myocytes isolated from these mice show a tendency to undergo mitochondrial swelling and spontaneous death [34], suggesting that the effects of Cyp D expression might be cell type-specific.

In contrast to the lack of any influence of Cyp D deficiency on apoptosis, the Cyp D-dependent MPT plays an important role in some forms of necrotic cell death (see Fig. 1). Cyp D-deficient MEFs show significantly increased resistance to H_2O_2-induced necrosis [33, 34], and Cyp D-deficient hepatocytes display resistance to necrosis induced by a Ca^{2+} ionophore (A23187) or by H_2O_2 [33, 34]. Interestingly, when H_2O_2-induced and Ca^{2+} ionophore-induced necrosis is inhibited by Cyp D deficiency in these cells, apoptosis does not occur as an alternate death mechanism [33], suggesting that the H_2O_2/Ca^{2+}-triggered apoptotic signaling pathways are somehow blocked in these types of cells.

Another very interesting question concerns the biological significance of the MPT because it is conceivable that the MPT plays a role in some physiological processes. By

analyzing Cyp D-deficient mice and cells in more detail, some hints about the role of the MPT should be obtained.

Regulation of the MPT by Bcl-2

Anti-apoptotic members of the Bcl-2 family, such as Bcl-2 itself and Bcl-x_L, are known to inhibit the Bax/Bak-dependent apoptotic increase of mitochondrial membrane permeability by direct interaction with pro-apoptotic members of this family, and also inhibit the MPT itself [39, 40] (see Fig. 1). How do these proteins block the MPT? Given that Bax/Bak is not essential for the MPT [33], Bcl-2 (Bcl-x_L) might directly inhibit a component of the PTP complex. In fact, Bcl-2 (Bcl-x_L) is capable of blocking VDAC activity [39] and ANT activity in liposome systems [41]. As described above, the VDAC plays a role in the MPT [29], whereas the ANT might not be important [31], so Bcl-2 and Bcl-x_L possibly inhibit the MPT by blocking the VDAC or unknown channels similar to the ANT that are actually involved in the MPT.

Role of the Cyp D-dependent MPT in disease

The advent of Cyp D-deficient mice has provided compelling evidence that the Cyp D-dependent MPT plays a crucial role in ischemia/reperfusion injury affecting the heart [33, 34] and brain [36], suggesting that the Cyp D-dependent MPT is involved in ischemia/reperfusion-induced cell death and that Cyp D and other components of the MPT are promising therapeutic targets. However, there have been a large number of reports published on the death mechanisms of ischemia/reperfusion injury and investigation of therapeutic methods, making it evident that ischemia/reperfusion injury is a very complex phenomenon which might involve multiple death mechanisms, because such injury can be suppressed by various inhibitors of different forms of cell death. It has been shown that ischemia/reperfusion injury can be ameliorated by inhibiting apoptosis with caspase inhibitors [42–45], inhibiting necroptosis with Nec1 [46], or blocking the Ask 1 pathway [47]. In studies of model systems employing cell lines, the death mechanisms involving caspases, a Nec1 target, Ask1, and the Cyp D-dependent MPT do not seem to overlap with each other. Why are so many different potential mechanisms involved in ischemia/reperfusion injury? Different death mechanisms might operate in the same cell in a sequential manner or in parallel, meaning that the inhibition of one mechanism might have a protective effect. Alternatively, different death mechanisms might act on different cells during ischemia/reperfusion injury and the dying cells might trigger the death process in other cells. It is also possible that different cell death mechanisms are activated by different ischemic conditions. For further studies of ischemia/reperfusion injury, mice that lack certain cell death mechanisms, such as Cyp D-deficient mice and Bax/Bak-deficient mice, would be useful tools.

The Cyp D-dependent MPT might also be involved in other diseases. It has been reported that mitochondria isolated from the livers of MND2 mice with mutation of the omi gene are more susceptible to the MPT [48]. MND2 mice succumb to motoneuron disease [49], which might be caused by the MPT occurring at a lower threshold in neuronal mitochondria. Thus, future studies may unveil a role of the Cyp D-dependent MPT in the pathogenesis of various diseases.

Acknowledgments The studies performed at our laboratory were partly supported by a grant for the 21st century COE Program, a grant for Scientific Research from the Ministry of Education, Science, Sports, and Culture of Japan, and a grant for Research on Dementia and Fracture from the Ministry of Health, Labour and Welfare of Japan.

References

1. Green DR, Evan GI (2002) A matter of life and death. Cancer Cell 1:19–30
2. Wang X (2001) The expanding role of mitochondria in apoptosis. Genes Dev 15:2922–2933
3. Desagher S, Martinou JC (2000) Mitochondria as the central control point of apoptosis. Trends Cell Biol 10:369–377
4. Tsujimoto Y (2003) Cell death regulation by the Bcl-2 protein family in the mitochondria. J Cell Physiol 195:158–167
5. Adams JM, Cory S (2001) Life-or-death decisions by the Bcl-2 protein family. Trends Biochem Sci 26:61–66
6. Kroemer G, Petit P, Zamzami N, Vayssiere JL, Mignotte B (1995) The biochemistry of programmed cell death. FASEB J 9:1277–1287
7. Zoratti M, Szabo I (1995) The mitochondrial permeability transition. Biochim Biophys Acta 1241:139–176
8. Halestrap AP, McStay GP, Clarke SJ (2002) The permeability transition pore complex: another view. Biochimie 84:153–166
9. Crompton M (2003) On the involvement of mitochondrial intermembrane junctional complexes in apoptosis. Curr Med Chem 10:1473–1484
10. He L, Lemasters JJ (2002) Regulated and unregulated mitochondrial permeability transition pores: a new paradigm of pore structure and function? FEBS Lett 512:1–7
11. Zamzami N, Kroemer G (2001) The michondrion in apoptosis: how Pandora's box opens. Nature Rev Mol Cell Biol 2:67–71
12. Galat A, Metcalfe SM (1995) Peptidylproline cis/trans isomerases. Prog Biophys Mol Biol 63:67–118
13. Broekemeier KM, Dempsey ME, Pfeiffer DR (1989) Cyclosporin A is a potent inhibitor of the inner membrane permeability transition in liver mitochondria. J Biol Chem 264:7826–7830
14. Green DR, Kroemer G (2004) The pathophysiology of mitochondrial cell death. Science 305:626–629
15. Zamzami N, Susin SA, Marchetti P, Hirsch T, Gomez-Monterrey I, Castedo M, Kroemer G (1996) Mitochondrial control of nuclear apoptosis. J Exp Med 183:1533–1544
16. Scorrano L, Ashiya M, Buttle K, Weiler S, Oakes SA, Mannella CA, Korsmeyer SJ (2002) A distinct pathway remodels mitochondrial cristae and mobilizes cytochrome *c* during apoptosis. Dev Cell 2:55–67

17. Newmeyer DD, Ferguson-Miller S (2003) Mitochondria: releasing power for life and unleashing the machineries of death. Cell 112:481–490
18. Szabo I, Zoratti M (1993) The mitochondrial permeability transition pore may comprise VDAC molecules. I. Binary structure and voltage dependence of the pore. FEBS Lett 330:201–205
19. Szabo I, De Pinto V, Zoratti M (1993) The mitochondrial permeability transition pore may comprise VDAC molecules. II. The electrophysiological properties of VDAC are compatible with those of the mitochondrial megachannel. FEBS Lett 330:206–210
20. Zizi M, Forte M, Blachly-Dyson E, Colombini M (1994) NADH regulates the gating of VDAC, the mitochondrial outer membrane channel. J Biol Chem 269:1614–1616
21. Gincel D, Zaid H, Shoshan-Barmatz V (2001) Calcium binding and translocation by the voltage-dependent anion channel: a possible regulatory mechanism in mitochondrial function. Biochem J 358(Pt 1):147–155
22. Gincel D, Shoshan-Barmatz V (2004) Glutamate interacts with VDAC and modulates opening of the mitochondrial permeability transition pore. J Bioenerg Biomembr 36:179–186
23. Pastorino JG, Shulga N, Hoek JB (2002) Mitochondrial binding of hexokinase II inhibits Bax-induced cytochrome *c* release and apoptosis. J Biol Chem 277:7610–7618
24. Pastorino JG, Hoek JB, Shulga N (2005) Activation of glycogen synthase kinase 3beta disrupts the binding of hexokinase II to mitochondria by phosphorylating voltage-dependent anion channel and potentiates chemotherapy-induced cytotoxicity. Cancer Res 65:10545–10554
25. Costantini P, Chernyak BV, Petronilli V, Bernardi P (1996) Modulation of the mitochondrial permeability transition pore by pyridine nucleotides and dithiol oxidation at two separate sites. J Biol Chem 271:6746–6751
26. Fontaine E, Eriksson O, Ichas F, Bernardi P (1998) Regulation of the permeability transition pore in skeletal muscle mitochondria. Modulation By electron flow through the respiratory chain complex i. J Biol Chem 1998 273:12662–12668
27. Pastorino JG, Hoek JB (2003) Hexokinase II: the integration of energy metabolism and control of apoptosis. Curr Med Chem 10:1535–1551
28. Crompton M, Virji S, Ward JM (1998) Cyclophilin-D binds strongly to complexes of the voltage-dependent anion channel and the adenine nucleotide translocase to form the permeability transition pore. Eur J Biochem 258:729–735
29. Shimizu S, Matsuoka Y, Shinohara Y, Yoneda Y, Tsujimoto Y (2001) Essential role of voltage-dependent anion channel in various forms of apoptosis in mammalian cells. J Cell Biol 152:237–250
30. Woodfield K, Ruck A, Brdiczka D, Halestrap AP (1998) Direct demonstration of a specific interaction between cyclophilin-D and the adenine nucleotide translocase confirms their role in the mitochondrial permeability transition. Biochem J 336:287–290
31. Kokoszka JE, Waymire KG, Levy SE, Sligh JE, Cai J, Jones DP, MacGregor GR, Wallace DC (2004) The ADP/ATP translocator is not essential for the mitochondrial permeability transition pore. Nature 427:461–465.
32. Shimizu S, Shinohara Y, Tsujimoto Y (2000) Bax and Bcl-xL independently regulate apoptotic changes of yeast mitochondria that require VDAC but not adenine nucleotide translocator. Oncogene 19:4309–4318
33. Nakagawa T, Shimizu S, Watanabe T, Yamaguchi O, Otsu K, Yamagata H, Inohara H, Kubo T, Tsujimoto Y (2005) Cyclophilin D-dependent mitochondrial permeability transition regulates some necrotic but not apoptotic death. Nature 434:652–658
34. Baines CP, Kaiser RA, Purcell NH, Blair NS, Osinska H, Hambleton MA, Brunskill EW, Sayen MR, Gottlieb RA, Dorn GW, Robbins J, Molkentin JD (2005) Loss of cyclophilin D reveals a critical role for mitochondrial permeability transition in cell death. Nature 434:658–662
35. Basso E, Fante L, Fowlkes J, Petronilli V, Forte MA, Bernardi P (2005) Properties of the permeability transition pore in mitochondria devoid of cyclophilin D. J Biol Chem 280:18558–18561
36. Schinzel AC, Takeuchi O, Huang Z, Fisher JK, Zhou Z, Rubens J, Hetz C, Danial NN, Moskowitz MA, Korsmeyer SJ (2005) Cyclophilin D is a component of mitochondrial permeability transition and mediates neuronal cell death after focal cerebral ischemia. Proc Natl Acad Sci USA 102:12005–12010
37. Lin DT, Lechleiter JD (2002) Mitochondrial targeted cyclophilin D protects cells from cell death by peptidyl prolyl isomerization. J Biol Chem 277:31134–31141
38. Schubert A, Grimm S (2004) Cyclophilin D, a component of the permeability transition pore, is an apoptosis repressor. Cancer Res 64:85–93
39. Shimizu S, Eguchi Y, Kamiike W, Funahashi Y, Mignon A, Lacronique V, Matsuda H, Tsujimoto Y (1998) Bcl-2 prevents apoptotic mitochondrial dysfunction by regulating proton flux. Proc Natl Acad Sci USA 95:1455–1459
40. Reed JC, Kroemer G (1998) The permeability transition pore complex: a target for apoptosis regulation by caspases and Bcl-2-related proteins. J Exp Med 187:1261–1271
41. Marzo I, Brenner C, Zamzami N, Jurgensmeier JM, Susin SA, Vieira HL, Prevost MC, Xie Z, Matsuyama S, Reed JC, Kroemer G (1998) Bax and adenine nucleotide translocator cooperate in the mitochondrial control of apoptosis. Science 281:2027–2031
42. Cheng Y, Deshmukh M, D'Costa A, Demaro JA, Gidday JM, Shah A, Sun Y, Jacquin MF, Johnson EM, Holtzman DM (1998) Caspase inhibitor affords neuroprotection with delayed administration in a rat model of neonatal hypoxic-ischemic brain injury. J Clin Invest 101:1992–1999
43. Chen J, Nagayama T, Jin K, Stetler RA, Zhu RL, Graham SH, Simon RP (1998) Induction of caspase-3-like protease may mediate delayed neuronal death in the hippocampus after transient cerebral ischemia. J Neurosci 18:4914–4928
44. Xu D, Bureau Y, McIntyre DC, Nicholson DW, Liston P, Zhu Y, Fong WG, Crocker SJ, Korneluk RG, Robertson GS (1999) Attenuation of ischemia-induced cellular and behavioral deficits by X chromosome-linked inhibitor of apoptosis protein overexpression in the rat hippocampus. J Neurosci 19:5026–5033
45. Bott-Flugel L, Weig HJ, Knodler M, Stadele C, Moretti A, Laugwitz KL, Seyfarth M (2005) Gene transfer of the pancaspase inhibitor P35 reduces myocardial infarct size and improves cardiac function. J Mol Med 83:526–534
46. Degterev A, Huang Z, Boyce M, Li Y, Jagtap P, Mizushima N, Cuny GD, Mitchison TJ, Moskowitz MA, Yuan J (2005) Chemical inhibitor of nonapoptotic cell death with therapeutic potential for ischemic brain injury. Nat Chem Biol 1:112–119
47. Watanabe T, Otsu K, Takeda T, Yamaguchi O, Hikoso S, Kashiwase K, Higuchi Y, Taniike M, Nakai A, Matsumura Y, Nishida K, Ichijo H, Hori M (2005) Apoptosis signal-regulating kinase 1 is involved not only in apoptosis but also in non-apoptotic cardiomyocyte death. Biochem Biophys Res Commun 333:562–527
48. Jones JM, Datta P, Srinivasula SM, Ji W, Gupta S, Zhang Z, Davies E, Hajnoczky G, Saunders TL, Van Keuren ML, Fernandes-Alnemri T, Meisler MH, Alnemri ES (2003) Loss of Omi mitochondrial protease activity causes the neuromuscular disorder of mnd2 mutant mice. Nature 425:721–727
49. Jones JM, Albin RL, Feldman EL, Simin K, Schuster TG, Dunnick WA, Collins JT, Chrisp CE, Taylor BA, Meisler MH (1993) mnd2: a new mouse model of inherited motor neuron disease. Genomics 16:669–677

THE JOURNAL OF BIOLOGICAL CHEMISTRY VOL. 282, NO. 22, pp. 16623–16630, June 1, 2007

A Bax/Bak-independent Mechanism of Cytochrome *c* Release*

Received for publication, December 1, 2006, and in revised form, March 6, 2007 Published, JBC Papers in Press, April 4, 2007, DOI 10.1074/jbc.M611060200

Takeshi Mizuta, Shigeomi Shimizu, Yousuke Matsuoka, Takashi Nakagawa, and Yoshihide Tsujimoto[1]

From the Laboratory of Molecular Genetics, Department of Medical Genetics, Osaka University Medical School, and Solution Oriented Research for Science and Technology (SORST) of the Japan Science and Technology Agency (JST), 2-2 Yamadaoka, Suita, Osaka 565-0871, Japan

Bax and Bak are multidomain pro-apoptotic members of the Bcl-2 family of proteins that regulate mitochondria-mediated apoptosis by direct modulation of mitochondrial membrane permeability. Since double-knock-out mouse embryonic fibroblasts with deficiency of Bax and Bak are resistant to multiple apoptotic stimuli, Bax and Bak are considered to be an essential gateway for various apoptotic signals. Here we showed that the combination of calcium ionophore A23187 and arachidonic acid induced cytochrome *c* release and caspase-dependent death of double-knock-out mouse embryonic fibroblasts, indicating that other mechanisms of cytochrome *c* release exist. Furthermore, A23187/arachidonic acid (ArA)-induced caspase-dependent death was significantly suppressed by the treatment of several serine protease inhibitors including 4-(2-aminoethyl)benzenesulfonylfluoride and L-1-chloro-3-(4-tosylamido)-4-phenyl-2-butanone but not the overexpression of anti-apoptotic Bcl-2 family of proteins or the inhibition of mitochondrial membrane permeability transition. These results indicate that there are at least two mechanisms of cytochrome *c* release leading to caspase activation, a Bax/Bak-dependent mechanism and a Bax/Bak-independent, but serine protease(s)-dependent, mechanism.

Apoptosis plays a critical role in the regulation of development processes, tissue homeostasis, and elimination of damaged cells. It has been shown that the mitochondria play a crucial role in apoptosis by releasing several apoptogenic molecules, such as cytochrome *c*, Smac/Diablo, and HtrA2/Omi (1, 2). After release into the cytosol, cytochrome *c* binds to Apaf-1 to cause recruitment of caspase-9, which leads to the initiation of a caspase cascade that includes caspase-3 and results in the occurrence of apoptotic cell death. Smac/Diablo and HtrA2/Omi bind directly with members of the inhibitor of apoptosis protein family, which are endogenous caspase inhibitory proteins and thus contribute to caspase activation (1, 2).

The best characterized regulators of apoptosis are the Bcl-2 family of proteins, which directly modulate outer mitochondrial membrane permeability during apoptosis. This family of proteins can be categorized into anti-apoptotic members (such as Bcl-2, Bcl-x_L, and Mcl-1) and pro-apoptotic members, which consist of multidomain proteins (such as Bax and Bak) and BH3-only proteins (including Bid, Bim, Bik, Bad, Noxa, and Puma) (3). The multidomain pro-apoptotic proteins Bax/Bak are essential and redundant regulators of a diverse intrinsic mitochondrial cell death pathway; Bax/Bak double-deficient murine embryonic fibroblasts (MEFs)[2] are resistant to multiple apoptotic stimuli that increase outer mitochondrial membrane permeability, including staurosporine, ultraviolet radiation, growth factor deprivation, and etoposide (4).

It was recently reported that double-knock-out (DKO) MEFs undergo death in a caspase-dependent manner, although at a lower rate when compared with WT MEFs, after exposure to agents such as arachidonic acid and Ca^{2+} ionophore (5), raising the possibility that there is a Bax/Bak-independent mechanism that regulates mitochondrial membrane permeability. In this present study, we found that the treatment of the combination of arachidonic acid and A23187 caused cytochrome *c* release and subsequently caspase activation succeeding the cell death in DKO MEFs. These events were inhibited by the treatment of 4-(2-aminoethyl)benzenesulfonylfluoride (AEBSF), a serine protease inhibitor, but not the treatment of mitochondrial permeability transition (mPT) inhibitors, deletion of cyclophilin D (mPT component), and overexpression Bcl-2 or Bcl-x_L.

EXPERIMENTAL PROCEDURES

Antibodies and Chemicals—The following antibodies were used. Numbers in parentheses indicate dilutions used. Anti-caspase-3 (1:250) and anti-caspase-9 (1:1000) monoclonal antibodies were purchased from BD Transduction Laboratories and MBL (Nagoya, Japan), respectively. Anti-lamin B1 (1:1000) and anti-GAPDH (1:1000) monoclonal antibodies were obtained from Zymed Laboratories Inc. Inc. (South San Francisco, CA) and BD Biosciences, respectively. Anti-cytochrome *c* monoclonal antibodies for Western blotting (clone 7H8.2C12, 1:1000) and immunostaining (clone 6H2.B4, 1:500) were purchased from Pharmingen. A23187 and arachidonic acid were obtained from Calbiochem and Sigma, respectively. AEBSF, L-1-chloro-3-(4-tosylamido)-4-phenyl-2-butanone (TPCK), and L-1-chloro-3-(4-tosylamido)-7-amino-2-heptanone (TLCK)

* The costs of publication of this article were defrayed in part by the payment of page charges. This article must therefore be hereby marked "*advertisement*" in accordance with 18 U.S.C. Section 1734 solely to indicate this fact.

[1] To whom correspondence should be addressed. Tel.: 81-6-6879-3363; Fax: 81-6-6879-3369; E-mail: tsujimot@gene.med.osaka-u.ac.jp.

[2] The abbreviations used are: MEF, murine embryonic fibroblast; DKO, double-knock-out; TKO, triple-knock-out; ArA, arachidonic acid; AEBSF, 4-(2-aminoethyl)benzenesulfonylfluoride; AEBSA, 4-(2-aminoethyl)benzenesulfonamide; TPCK, L-1-chloro-3-(4-tosylamido)-4-phenyl-2-butanone; TLCK, L-1-chloro-3-(4-tosylamido)-7-amino-2-heptanone; WT, wild type; mPT, mitochondrial permeability transition; GAPDH, glyceraldehyde-3-phosphate dehydrogenase; DFP, diisopropylfluorophosphate; GFP, green fluorescent protein; siRNA, small interfering RNA; PBS, phosphate-buffered saline; CsA, cyclosporin A; Cyp D, cyclophilin D; Z, benzyloxycarbonyl; fmk, fluoromethyl ketone; Ac, acetyl; MCA, methylcoumarylamide.

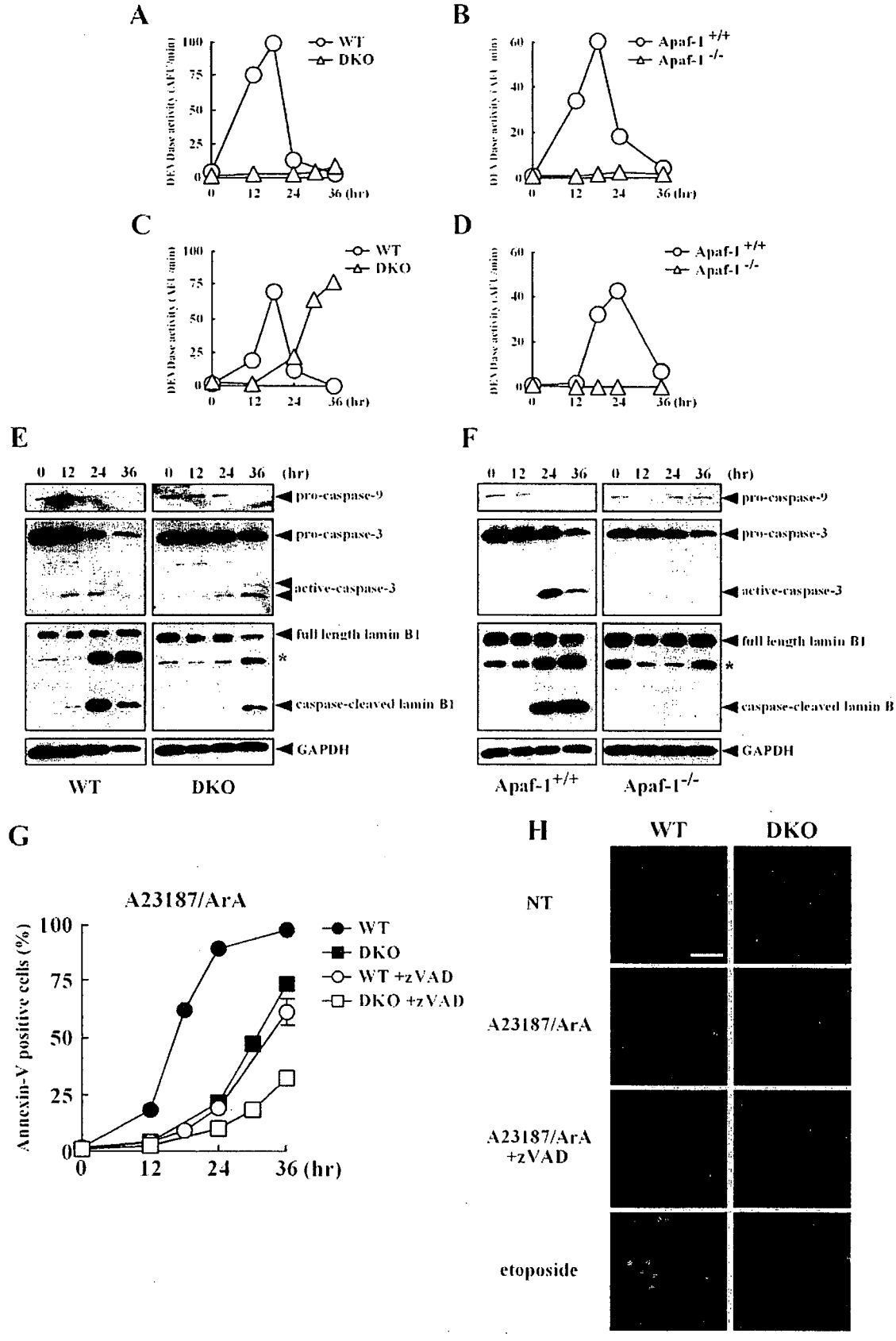

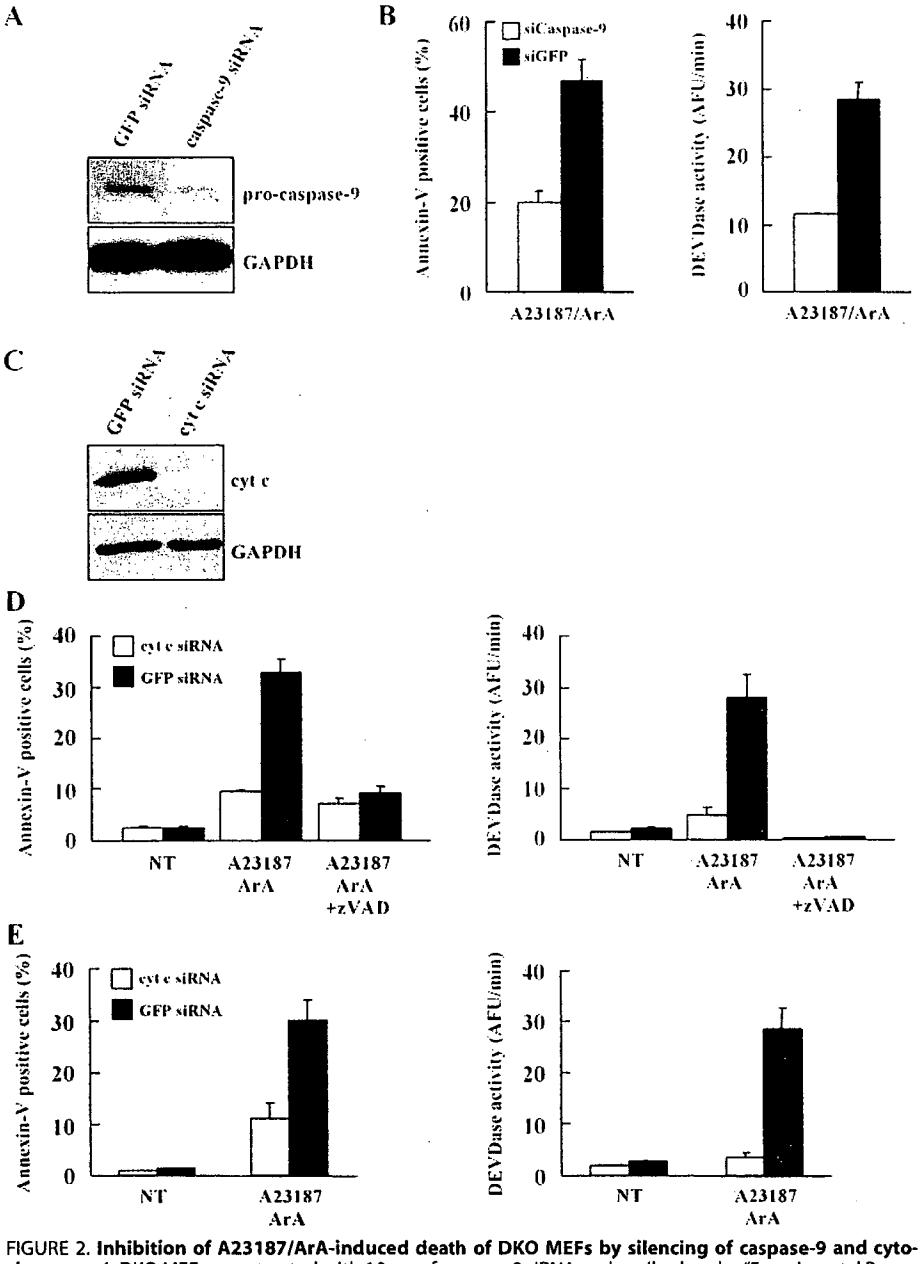

FIGURE 2. **Inhibition of A23187/ArA-induced death of DKO MEFs by silencing of caspase-9 and cytochrome *c*.** *A*, DKO MEFs were treated with 10 μg of caspase-9 siRNA as described under "Experimental Procedures," after which the expression of caspase-9 and GAPDH (loading control) was analyzed by Western blotting. *B*, DKO MEFs with silencing of caspase-9 (*siCaspase-9*) were treated with 10 μM A23187 plus 100 μM ArA for 24 h, and then the extent of cell death (defined by annexin V staining) and DEVDase activity was measured (n = 4). *siGFP*, silencing of GFP. *C*, DKO MEFs were treated with 5 μg of cytochrome *c* siRNA. Expression of cytochrome *c* (*cyt c*) and GAPDH was analyzed. *D* and *E*, DKO MEFs with silencing of cytochrome *c* were treated with A23187/ArA in the absence or presence of 100 μM Z-VAD-fmk for 24 h. *NT*, not treated. *E*, the same experiments as shown in *D* were performed, except in the presence of 1 μM antimycin A for 12 h. Cell death (defined by annexin-V staining) and DEVDase activity were measured (n = 4).

were purchased from Roche Applied Science (Penzberg, Germany). 4-(2-Aminoethyl)benzenesulfonamide (AEBSA) were purchased from Aldrich (Steinheim, Germany). Diisopropylfluorophosphate (DFP) and other chemicals were purchased from Wako Co. (Osaka, Japan).

Cell Culture and DNA Transfection—SV40 T antigen-immortalized WT MEFs, Bax/Bak DKO MEFs (kindly provided by Dr. S. J. Korsmeyer), and Bax/Bak/CypD TKO MEFs were grown in Dulbecco's minimal essential medium supplemented with 10% fetal bovine serum. Apaf-1-deficient MEFs and control MEFs were kindly provided by Dr. X. Wang and were also grown in the same medium. DNAs encoding human Bax and human Bcl-x_L were used in the pUC-CAGGS expression vector. Cells (1×10^6) were transfected with plasmid DNA using the Amaxa electroporation system according to the supplier's protocol (kit V, program U-20). The transfection efficiency was more than 75% as assessed by co-transfection with DNA expressing green fluorescence protein (GFP). All of the siRNAs were produced by Dharmacon Research. The sequences used were as follows (numbers in parentheses indicate nucleotide positions within the respective open reading frames): mouse cytochrome *c* siRNA, 5′-GGGAGAAAGGGCAGACCUA-3′ (267–285); mouse HtrA2/Omi siRNA, 5′-GGGGAGUUUGUUGUUGCCA-3′ (760–778); and GFP siRNA, 5′-GGCUACGUCCAGGAGCGCA-3′ (274–292). Mouse caspase-9 siRNA SMARTpool™ was also purchased from Dharmacon Research. Cells (1×10^6) were transfected twice on alternate days with 10 μg of siRNA using the Amaxa electroporation system.

FIGURE 1. **Induction of caspase-dependent death of DKO MEFs by A23187/ArA.** *A–D*, activation of DEVDase in MEFs exposed to death stimuli. WT MEFs and DKO MEFs (*A* and *C*) or Apaf-$1^{+/+}$ and Apaf-$1^{-/-}$ MEFs (*B* and *D*) were treated with 10 μM etoposide (*A* and *B*) and 10 μM A23187 plus 100 μM arachidonic acid (*C* and *D*), and DEVDase activity was measured. Representative results from three independent experiments are shown. *E* and *F*, activation of caspases in DKO MEFs, but not in Apaf-$1^{-/-}$ MEFs, by A23187/ArA. The indicated MEFs were incubated with A23187/ArA for the indicated times. Cleavage of pro-caspase-9, pro-caspase-3, and lamin B1 was analyzed by Western blotting. GAPDH was also analyzed as a loading control. *, nonspecific band. *G* and *H*, induction of death in A23187/ArA-treated DKO MEFs. WT and DKO MEFs were not treated (*NT*) or were treated with A23187/ArA in the presence or absence of 100 μM Z-VAD-fmk (*G* and *H*) or 10 μM etoposide (*H*) for 36 h. The extent of cell death was assessed by annexin V staining (*G*). Data are shown as the mean ± S.D. (n = 4). Representative nuclear morphology is shown (*H*). *Bars*, 50 μm.

Twenty-four hours after the second transfection with siRNA, cells were used for experiments.

Cell Viability and DEVDase Activity Assay—Cells (2×10^5/well) were seeded into 6-well dishes. After 24 h, the cells were treated with 10 μM A23187/100 μM arachidonic acid or 10 μM etoposide in the presence or absence of 100 μM Z-VAD-fmk or 100 μg/ml AEBSF. Cells were harvested and stained with 1 μM propidium iodide, 1 μM Cy3-conjugated annexin V, or 1 μM Hoechst 33342 for 5 min at room temperature and were analyzed with a flow cytometer (BD Biosciences, FACS Caliber) or under a fluorescence microscope (Olympus, BX50). For DEVDase assay, cells were washed three times with phosphate-buffered saline (PBS) and suspended in 50 mM Tris-HCl (pH 7.4), 1 mM EDTA, and 10 mM EGTA. After the addition of Triton-X to 0.1%, cells were incubated for 30 min at on ice. Lysates were clarified by centrifugation at 8000 rpm for 3 min, and cleared lysates containing 50 μg of protein were incubated with 100 μM enzyme substrate Ac-DEVD-MCA at 37 °C for 1 h. Levels of released 7-amino-4-methlycoumarin were measured using a spectrofluorometer (Hitachi F-3000) with excitation at 380 nm and emission at 460 nm.

Preparation of the Cytosolic Fraction and Total Cell Lysate—For the detection of released cytochrome *c*, the cytosolic fraction was collected from MEFs after incubation with 0.1 mg/ml digitonin for 5 min at 37 °C in isotonic buffer (20 mM potassium-Hepes (pH 7.4), 10 mM KCl, 1.5 mM $MgCl_2$, 250 mM sucrose, and 1 mM Na^{2+}-EDTA). After centrifugation at 8000 rpm for 5 min, aliquots of the supernatant (cytosolic fraction) and the pellet (mitochondrial fraction) were analyzed by Western blotting with an anti-cytochrome *c* antibody. In some experiments, cells were lysed with radioimmune precipitation assay buffer (50 mM Tris-HCl (pH 8.0), 0.1% SDS, 1% Nonidet P-40, 0.5% deoxycholate (sodium salt), and 150 mM NaCl).

Immunofluorescence Staining—Cells were fixed in 4% paraformaldehyde for 30 min and then permeabilized with 0.1% Triton X-100 for 15 min at room temperature. After incubation with 2% fetal bovine serum in PBS for 1 h, the cells were incubated with anti-cytochrome *c* for 1 h. After washing three times with PBS, the cells were incubated with the secondary antibody (Alexa Fluor 488-conjugated anti-mouse IgG, 1:1000) for 1 h. Then fluorescence was detected under a confocal microscope (Zeiss, LSM 510).

Microinjection—DKO MEFs (1.5×10^4) were plated on 35-mm dishes 1 day before use. PBS or PBS containing 400 μM AEBSF, 400 μM AEBSA, 100 μM DFP, 100 μM TLCK, or 200 μM TPCK was microinjected through a glass capillary into the cytoplasm with a Narishige micromanipulator. For identification of injected cells, samples were mixed with green fluorescent protein. Cells were then treated with A23187/ArA at 1 h. Cell morphology was examined 20 h after A23187/ArA treatment under a fluorescence microscope.

RESULTS

We added various apoptotic reagents to Bax/Bak DKO MEFs, Apaf-$1^{-/-}$ MEFs, and their control MEFs, all of which were immortalized, and then measured DEVDase activity. In both DKO MEFs (Fig. 1*A*) and Apaf-$1^{-/-}$ MEFs (Fig. 1*B*), activation of DEVDase was not observed after exposure to etoposide that induced mitochondria-mediated apoptosis, whereas in the control MEFs, activation of DEVDase was readily observed, confirming previous observations that Bax/Bak is essential for such apoptosis (4, 6). Time-dependent decrease of DEVDase activities was due to disruption of plasma membrane. Similar results were also obtained when these cells were treated with staurosporine, UV, and X-rays (data not shown). In contrast, when the cells were treated with A23187 plus ArA, activation of DEVDase was observed in DKO MEFs but not in Apaf-$1^{-/-}$ MEFs (Fig. 1, *C* and *D*). It has previously been reported that ionomycin (another Ca^{2+} ionophore) plus ArA could induce DEVDase activation in DKO MEFs (5). Consistent with the elevation of caspase activation, A23187/ArA treatment induced cleavage of caspase-9, caspase-3, and lamin B1 in WT and DKO MEFs but not in Apaf-$1^{-/-}$ MEFs (Fig. 1, *E* and *F*). Furthermore, A23187/ArA induced the death of DKO MEFs, as assessed by staining with annexin V (Fig. 1*G*) and propidium iodide (data not shown), whereas such cell death was not completely inhibited by Z-VAD-fmk, a pan-caspase inhibitor (Fig. 1*G* and data not shown), indicating that A23187/ArA induced both caspase-dependent and caspase-independent death of DKO MEFs. It is known that not a few reagents induce both apoptosis and necrosis, such as oxidative stress (7) and Ca^{2+} overload (8). Staining with Hoechst 33342 revealed that A23187/ArA induced nuclear pyknosis, which was partially inhibited by Z-VAD-fmk (Fig. 1*H*). A23187/ArA-induced caspase activation and death of DKO MEFs were slightly delayed when compared with these processes in WT MEFs (Fig. 1, *C* and *G*). Primary cultures of DKO MEFs tended to mainly

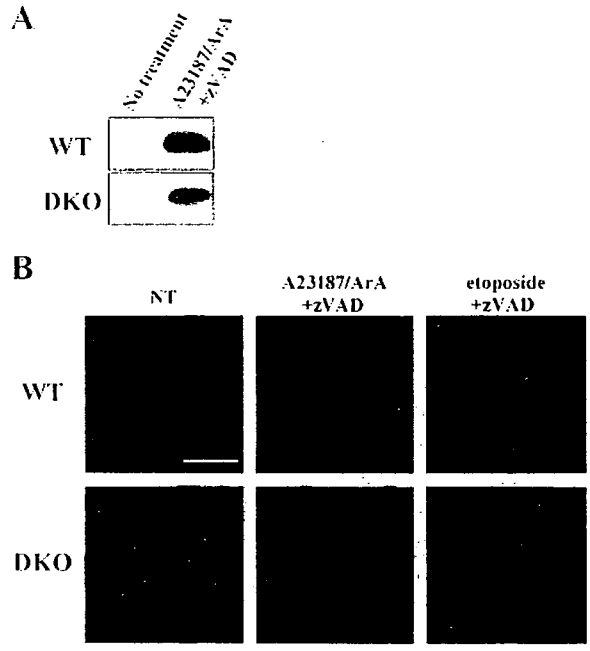

FIGURE 3. **Cytochrome c release in A23187/ArA-treated MEFs.** WT and DKO MEFs were not treated (*NT*) or were treated with 10 μM A23187 plus 100 μM ArA in the presence of Z-VAD-fmk (100 μM). *A*, after 18 h, the cytoplasmic fraction was recovered, and samples were subjected to Western blotting for detection of cytochrome *c*. *B*, after 12 h, MEFs were fixed and immunostained with an anti-cytochrome c monoclonal antibody. In *B*, MEFs were also treated with 10 μM etoposide plus 100 μM Z-VAD-fmk. *Bars*, 50 μm.

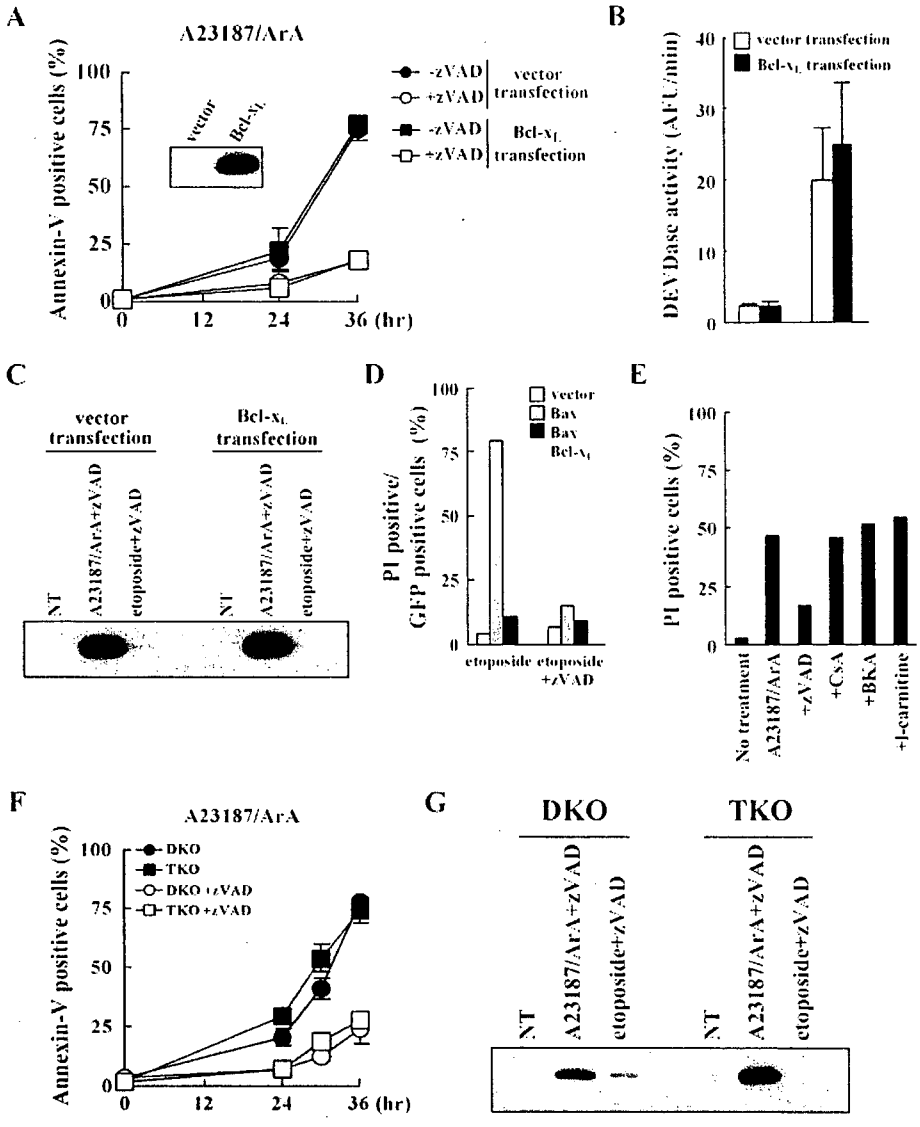

FIGURE 4. **No effect of Bcl-x_L or inhibition of the permeability transition on A23187/ArA-induced death of DKO MEFs.** *A* and *B*, overexpression of Bcl-x_L did not affect A23187/ArA-induced death of DKO MEFs. Cells were transfected with the indicated plasmids (0.5 μg). After 24 h, the cells were incubated with 10 μM A23187 plus 100 μM ArA in the presence or absence of 100 μM Z-VAD-fmk. Cell death (defined by annexin V staining) (*A*) and DEVDase activity at 24 h (*B*) were measured ($n = 4$). *C*, overexpression of Bcl-x_L did not affect A23187/ArA-induced cytochrome *c* release in DKO MEFs. DKO MEFs with or without Bcl-x_L overexpression were incubated with A23187/ArA in the presence of 100 μM Z-VAD-fmk for 18 h. Then the cytoplasmic and mitochondrial fractions were recovered, and samples were subjected to Western blotting for detection of cytochrome *c*. *NT*, not treated. *D*, Bcl-x_L inhibited Bax-induced apoptosis. DKO MEFs were transfected with plasmids expressing Bax, Bcl-x_L, or control vector together with a GFP-expressing plasmid. After 24 h, cells were treated with 100 μM etoposide in the presence or absence of 100 μM Z-VAD-fmk for another 24 h. Cell death was determined by counting the propidium iodide (*PI*)-positive cells among GFP-positive cells. *E*, mPT inhibitors failed to inhibit A23187/ArA-induced death of DKO MEFs. Cells were treated with A23187/ArA in the presence of 100 μM Z-VAD-fmk or several mPT inhibitors (1 μM CsA, 10 μM bongkrekic acid (*BKA*), or 2 mM L-carnitine). After 24 h, cell death was assessed by propidium iodide staining. *F*, lack of Cyp D did not influence A23187/ArA-induced death of DKO MEFs. DKO MEFs (Bax/Bak-deficient) and TKO MEFs (Bax/Bak/Cyp D-deficient) were incubated with A23187/ArA in the presence or absence of 100 μM Z-VAD-fmk. Then cell death was assessed by annexin V staining ($n = 4$). *G*, lack of Cyp D did not affect A23187/ArA-induced cytochrome *c* release. The same experiment as in *C* was performed, except for the use of TKO MEFs and DKO MEFs.

undergo caspase-independent death (data not shown). These results indicated that A23187/ArA induced caspase-dependent death of immortalized MEFs in both a Bax/Bak-dependent and a Bax/Bak-independent manner.

To examine whether mitochondria were involved in the A23187/ArA-induced caspase-dependent death of DKO MEFs, we used gene silencing with siRNA to down-regulate caspase-9 and cytochrome *c*. Caspase-9 is activated by forming a complex called the apoptosome with Apaf-1 and cytochrome *c* in the presence of (d)ATP (9). Proteolytic activation of caspase-9 leads to activation of caspase-3 (9). Endogenous caspase-9 and cytochrome *c* were silenced in DKO MEFs by the respective siRNAs (Fig. 2, *A* and *C*). Silencing of caspase-9 and cytochrome *c* in DKO MEFs markedly reduced A23187/ArA-induced death, as assessed by annexin V staining, but did not completely abolish it (Fig. 2, *B* and *D*). Although silencing of caspase-9 only partially inhibited the activation of DEVDase (Fig. 2*B*), probably due to incomplete silencing (Fig. 2*A*), silencing of cytochrome *c* inhibited more strongly the activation of DEVDase (Fig. 2*D*). These results indicated that A23187/ArA-induced caspase activation required the presence of Apaf-1/cytochrome *c*. Incomplete inhibition of cell death after silencing of cytochrome *c* was mainly due to the simultaneous occurrence of caspase-independent death because the addition of Z-VAD-fmk did not further reduce A23187/ArA-induced death, as shown in Fig. 2*D*. To avoid the influence of mitochondrial respiration in the experiment with silencing of cytochrome *c*, we also performed the experiment in the presence of antimycin A (an inhibitor of respiration) and, although antimycin A enhanced cell death, virtually identical results were obtained (Fig. 2*E*). These results indicated that A23187/ArA-induced caspase-dependent death required the presence of Apaf-1/caspase-9/cytochrome *c* but not Bax/Bak.

We next examined whether cytochrome *c* was released from the mitochondria in A23187/ArA-treated DKO MEFs. Subcellular fractionation revealed that etoposide induced cytochrome *c* release in WT MEFs but not DKO MEFs (data not shown), whereas A23187/ArA caused cytochrome *c* release from both

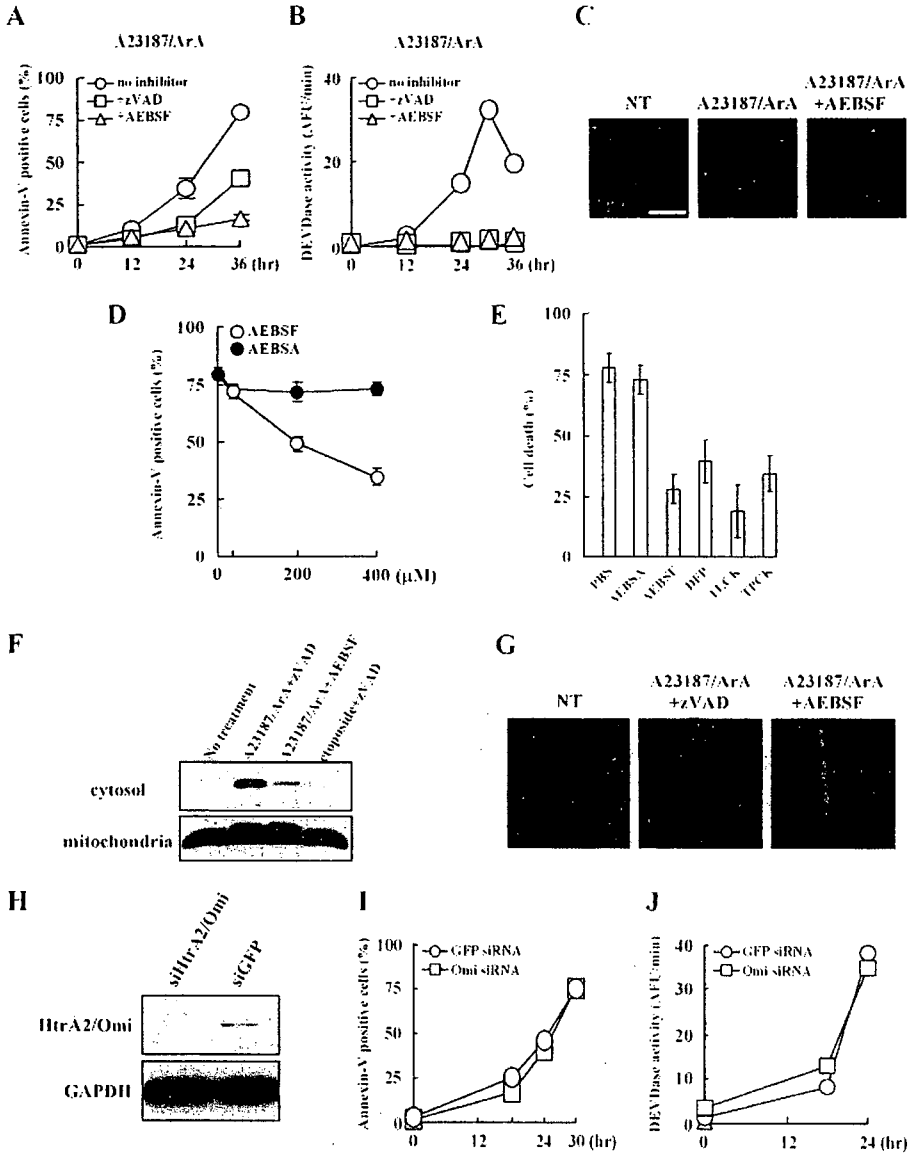

FIGURE 5. **Inhibition of A23187/ArA-induced cell death of DKO MEFs by the treatment of serine protease inhibitors.** *A–C*, inhibition of A23187/ArA-induced cell death of DKO MEFs by AEBSF. Cells were incubated with 10 μM A23187 plus 100 μM ArA in the presence or absence of 100 μM Z-VAD-fmk or 100 μg/ml AEBSF. Then cell death (defined by annexin V staining) (*A*) and DEVDase activity (*B*) were measured ($n = 4$). Representative nuclear morphology of A23187/ArA-treated DKO MEFs in the presence or absence of AEBSF at 24 h is shown in *C*. *NT*, not treated. *Bars*, 50 μm. *D*, inhibition of A23187/ArA-induced cell death by AEBSF but not AEBSA, an inactive analog. DKO MEFs were incubated with A23187/ArA in the presence of 40, 200, and 400 μM AEBSF or AEBSA. After 30 h, the extent of cell death was assessed by annexin V staining. Data are shown as the mean ± S.D. ($n = 3$). *E*, inhibition of A23187/ArA-induced cell death by various serine protease inhibitors. Serine protease inhibitors, AEBSF, DFP, TLCK, and TPCK or the negative control (AEBSA and PBS) were microinjected into the DKO MEFs with GFP as described under "Experimental Procedures." After 1 h, cells were treated with A23187/ArA, and the cell death was assessed after 20 h. Cell viability was determined by counting GFP-positive cells attached on the dish among total injected GFP-positive cells. Data are shown as the mean ± S.D. ($n = 3$). *F* and *G*, inhibition of A23187/ArA-induced cytochrome *c* release by AEBSF. DKO MEFs were not treated or were treated with A23187/ArA in the presence of Z-VAD-fmk (100 μM) or AEBSF (100 μg/ml) for 18 (*F*) or 12 h (*G*). In *F*, the cytoplasmic fraction was recovered, and samples were subjected to Western blotting for detection of cytochrome *c*. In *G*, MEFs were fixed and immunostained with an anti-cytochrome *c* monoclonal antibody. *H–J*, no inhibition of A23187/ArA-induced cell death by silencing of HtrA2/Omi, a mitochondrial serine protease, was shown. *H*, DKO MEFs were treated with 10 μg of HtrA2/Omi siRNA as described under "Experimental Procedures," after which the expression of HtrA2/Omi and GAPDH (loading control) was analyzed by Western blotting. DKO MEFs with silencing of HtrA2/Omi or GFP (control) were treated with A23187/ArA, after which cell death (defined by annexin-V staining) (*I*) and DEVDase activity (*J*) were measured ($n = 4$).

WT and DKO MEFs in the presence of Z-VAD-fmk (Fig. 3*A*). Consistent with this result, cytochrome *c* localization was altered in A23187/ArA-treated DKO MEFs, but not etoposide-treated DKO MEFs, as assessed by immunofluorescence microscopy (Fig. 3*B*). All these findings indicated that A23187/ArA induced cytochrome *c* release in a Bax/Bak-independent manner and subsequently activated caspases to induce cell death.

How was cytochrome *c* released from the mitochondria in a Bax/Bak-independent manner after treatment with A23187/ArA? First, we examined whether Bcl-x_L could inhibit this Bax/Bak-independent process of cytochrome *c* release. As shown in Fig. 4*A*, a pan-caspase inhibitor, but not overexpression of Bcl-x_L, inhibited A23187/ArA-induced death of DKO MEFs. Consistent with this result, activation of both caspases and cytochrome *c* release was not influenced by Bcl-x_L (Fig. 4, *B* and *C*). As expected, the expression of Bcl-x_L markedly inhibited etoposide-induced apoptosis in Bax-transfected DKO MEFs (Fig. 4*D*).

ArA and Ca^{2+} ionophore A23187 are thought to induce the mPT (8, 10, 11), which is a Ca^{2+}-dependent, cyclosporin A (CsA)-sensitive increase of mitochondrial membrane permeability that allows various solutes to equilibrate across the membranes (12). Since the CsA-sensitive mPT has been suggested to have a role in apoptotic cytochrome *c* release, we investigated whether it was also involved in A23187/ArA-induced Bax/Bak-independent cytochrome *c* release and cell death. Accordingly, CsA, bongkrekic acid, and L-carnitine, all of which are known to inhibit the mPT (12, 13), were added to cultures of A23187/ArA-treated DKO MEFs. As shown in Fig. 4*E*, none of these reagents inhibited A23187/ArA-induced death, whereas Z-VAD-fmk caused significant inhibition, suggesting that the mPT was not involved in this mode of cell death. To confirm this possibility,

we employed mice lacking cyclophilin D (Cyp D), in which the CsA-sensitive mPT is completely blocked (14). Cross-breeding produced $Bax^{-/-}Bak^{-/-}$Cyp $D^{-/-}$ (TKO) mice, from which immortalized MEFs were obtained. As shown in Fig. 4*F*, A23187/ArA equally induced the death of TKO and DKO MEFs, with cell death being partially inhibited by Z-VAD-fmk. Consistent with these findings, cytochrome *c* release was also observed in A23187/ArA-treated TKO MEFs (Fig. 4*G*), indicating that the CsA-sensitive mPT was not involved in Bax/Bak-independent cytochrome *c* release and cell death induced by A23187/ArA.

To obtain some insight into the molecular mechanisms of A23187/ArA-induced cytochrome *c* release, we tested the effects of various drugs, such as protease inhibitors and lipase inhibitors, on A23187/ArA-treated DKO MEFs and found that AEBSF, which inhibits serine proteases through sulfonylation of the active site serine residue (15) and has been described to inhibit some forms of cell death (16–19), could prevent A23187/ArA-induced caspase activation and cell death (Fig. 5, *A–C*). AEBSF inhibited A23187/ArA-induced cell death in a dose-dependent manner, whereas AEBSA, an inactive analog of AEBSF, did not inhibit it at any doses tested (Fig. 5*D*). To confirm the involvement of a serine protease(s), we examined other serine protease inhibitors, DFP, TLCK, and TPCK. The addition of DFP, TLCK, and TPCK into culture medium did not inhibit A23187/ArA-induced death (data not shown), which could be due to their membrane impermeability; therefore, we microinjected them into cells. As shown in Fig. 5*E*, all the serine protease inhibitors inhibited A23187/ArA-induced cell death. Since inhibitors are diluted to 2.5×10^2-10^3-fold in the cytoplasm (20), the estimated intracellular concentrations of AEBSF are calculated to 40–400 nM. AEBSF not only inhibited A23187/ArA-induced cell death but also blocked cytochrome *c* release (Fig. 5, *F* and *G*). These results indicated that a serine protease(s) is involved in the process of A23187/ArA-induced cell death upstream of cytochrome *c* release. AEBSF was a more effective inhibitor of A23187/ArA-induced cell death than Z-VAD-fmk (Fig. 5*A*), suggesting that it acted at a common step further upstream in the death-signaling pathways or that it inhibited independently both caspase-dependent and caspase-independent cell death. We examined the influence of HtrA2/Omi, a serine protease located in the mitochondria that is known to be involved in apoptosis (21, 22). As shown in Fig. 5, *H–J*, silencing of HtrA2/Omi had no effect on A23187/ArA-induced death, although it significantly reduced Fas-mediated apoptosis of DKO MEFs (data not shown).

DISCUSSION

This study revealed the following findings. 1) the combination of Ca^{2+} ionophore A23187 and arachidonic acid causes caspase-dependent cell death following cytochrome *c* release as well as caspase-independent death in Bax/Bak double-knock-out MEFs. 2) The Bcl-2 family of proteins and the CsA-sensitive mPT are not involved in this mode of cell death. 3) Instead, this mode of death is mediated by an unknown serine protease(s). These findings demonstrate the existence of a novel mechanism of cytochrome *c* release that is regulated by serine proteases but not by the Bcl-2 family.

Bax/Bak-dependent and Bax/Bak-independent mechanisms seem to respond to different stimuli. After treatment with etoposide, UV, or staurosporine, cytochrome *c* release occurred in a Bcl-2 family-dependent manner, whereas A23187/ArA not only induced cytochrome *c* release in a Bcl-2 family-dependent manner but also in a Bcl-2 family-independent, serine protease(s)-dependent manner. This difference might be related to the influence of molecule(s) acting upstream of the mitochondria. Since apoptosis induced by BH3-only proteins occurs in a Bax/Bak-dependent manner (23, 24), A23187/ArA probably activates unidentified apoptotic molecule(s) in addition to BH3-only proteins. A23187/ArA interferes with intracellular Ca^{2+} homeostasis (5), so Ca^{2+} itself or Ca^{2+}-regulated proteins might be involved in the mechanism of A23187/ArA-induced cell death. If the Ca^{2+} ion was a major signal mediator, it seemed likely that cytochrome *c* release would occur via mPT. However, we excluded this possibility by employing MEFs deficient in Bax, Bak, and Cyp D (Fig. 4, *F* and *G*). This result was consistent with our findings obtained in Cyp $D^{-/-}$ MEFs and mice (14) that cell death mediated via the mPT is necrosis but not apoptosis, probably due to the decline of ATP caused by $\Delta\psi$ loss. Therefore, a Ca^{2+}-regulated protein, rather than Ca^{2+} itself, may be the most suitable candidate as an inducer of Bax/Bak-independent cytochrome *c* release. We could not formally exclude the possibility that A23187/ArA-induced cytochrome *c* release was mediated by the CsA-insensitive mPT.

Since A23187/ArA-induced death of DKO MEFs was inhibited by the treatment of serine protease inhibitors including AEBSF and TPCK, proteolytic activity of a serine protease(s) seems to be involved in this form of cell death. Although it is still to be determined how serine protease inhibitors suppressed A23187/ArA-induced death, the possibility was excluded that AEBSF inhibited A23187/ArA-induced death by blocking mitochondrial Ca^{2+} uptake, by using Rhod2-AM as an indicator of mitochondrial Ca^{2+} uptake.[3] A serine protease(s) may cleave one or more unidentified substrates in the mitochondria that are involved in the regulation of death due to A23187/ArA. For example, a mitochondrial channel protein might be cleaved by a serine protease(s), resulting in conformational changes that allow cytochrome *c* release, but elucidation of the actual mechanism will require further investigation.

A serine protease(s)-mediated, but not Bax/Bak-mediated, cytochrome *c* release and caspase-dependent cell death were observed in immortalized MEFs. Do other normal cells also have the potential to undergo these forms of death? It has previously been described that the brains of $bax^{-/-}bak^{-/-}$ mice displayed a normal gross anatomy, regardless of the fact that neuronal progenitor cells derived from these mice are strongly resistant to apoptosis (25, 26). Note that mature neurons present in cerebellar granule cell cultures from $bax^{-/-}bak^{-/-}$ mice are as sensitive to excitotoxic cell death

[3] T. Mizuta, S. Shimizu, and Y. Tsujimoto, unpublished results.